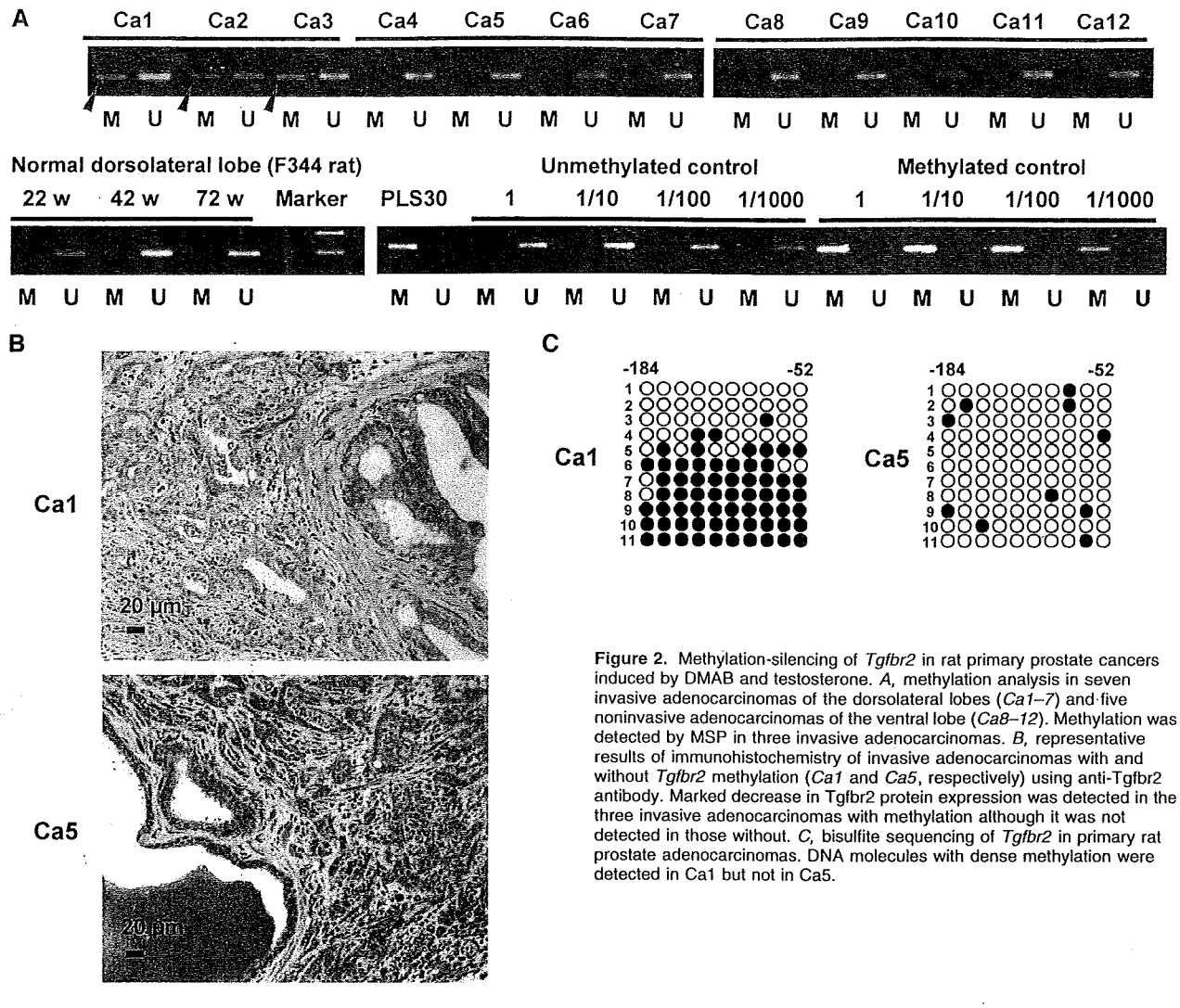

Figure 2. Methylation-silencing of *Tgfbr2* in rat primary prostate cancers induced by DMAB and testosterone. *A*, methylation analysis in seven invasive adenocarcinomas of the dorsolateral lobes (*Ca1–7*) and five noninvasive adenocarcinomas of the ventral lobe (*Ca8–12*). Methylation was detected by MSP in three invasive adenocarcinomas. *B*, representative results of immunohistochemistry of invasive adenocarcinomas with and without *Tgfbr2* methylation (*Ca1* and *Ca5*, respectively) using anti-Tgfbr2 antibody. Marked decrease in Tgfbr2 protein expression was detected in the three invasive adenocarcinomas with methylation although it was not detected in those without. *C*, bisulfite sequencing of *Tgfbr2* in primary rat prostate adenocarcinomas. DNA molecules with dense methylation were detected in Ca1 but not in Ca5.

a *Sac*I-*Bam*HI fragment that contained *TGFBR2* promoter and luciferase cDNA was recovered after electrophoresis in an agarose gel.

Along with a control plasmid for transfection efficiency (3 ng phRL-TK; Promega), 30 ng of the *Sac*I-*Bam*HI fragment was transiently transfected into PC3 cells using Lipofectamine 2000 transfection reagent (Invitrogen) with Opti-MEM I Reduced-Serum Medium (Invitrogen) in a 96-well format. At 24 h after transfection, cells were harvested, and luciferase activity was measured with the Dual-Luciferase Reporter Assay System (Promega) in a Lumat LB 9507 (Berthold Technologies). Each transfection and measurement was performed in triplicate.

Sequencing analysis for mutation analysis of human *TGFBR2*. The polyadenylic acid tract in exon 3 of *TGFBR2* (nucleotides 831–840 of NM_001024847), the target region of microsatellite instability (25), was amplified using Phusion high-fidelity DNA polymerase with HF Buffer (New England Biolabs). The product was sequenced with inner primers (Supplementary Table S2).

Results

Genes up-regulated by 5-aza-dC treatment and their methylation analysis. Three rat prostate cancer cell lines (PLS10, PLS20, and PLS30) were treated with 10 μmol/L of 5-aza-dC, and up-regulated genes were searched for using an oligonucleotide microarray. Among >28,000 genes and expressed sequence tags analyzed by the microarray, 47, 13, and 10 annotated genes (59 nonredundant annotated genes), respectively, were up-regulated at 16-fold or more (signal log ratio ≥4) in the three cell lines (Supplementary Tables S3 and S4). The presence of a putative promoter CGI was examined by a database search, and 10, 3, and 1 genes (12 nonredundant genes) were found to have CGIs that spanned 300 bp or more (Supplementary Table S3). Genes with these CGIs were considered as candidates for novel methylation-silenced genes in rat prostate cancers.

To examine whether the induction of these genes by 5-aza-dC treatment was due to demethylation of promoter CGIs, the methylation statuses of the putative promoter CGIs were analyzed by MSP. The CGIs of eight genes (*Aebp1, Dysf, Gas6, LOC361288, Nnat, Ocm, RGD1308119*, and *Tgfbr2*) were completely methylated before the treatment and demethylated after the treatment in at least one of the three rat prostate cancer cell lines (Table 1). The up-regulation of mRNA expression of these eight genes detected by

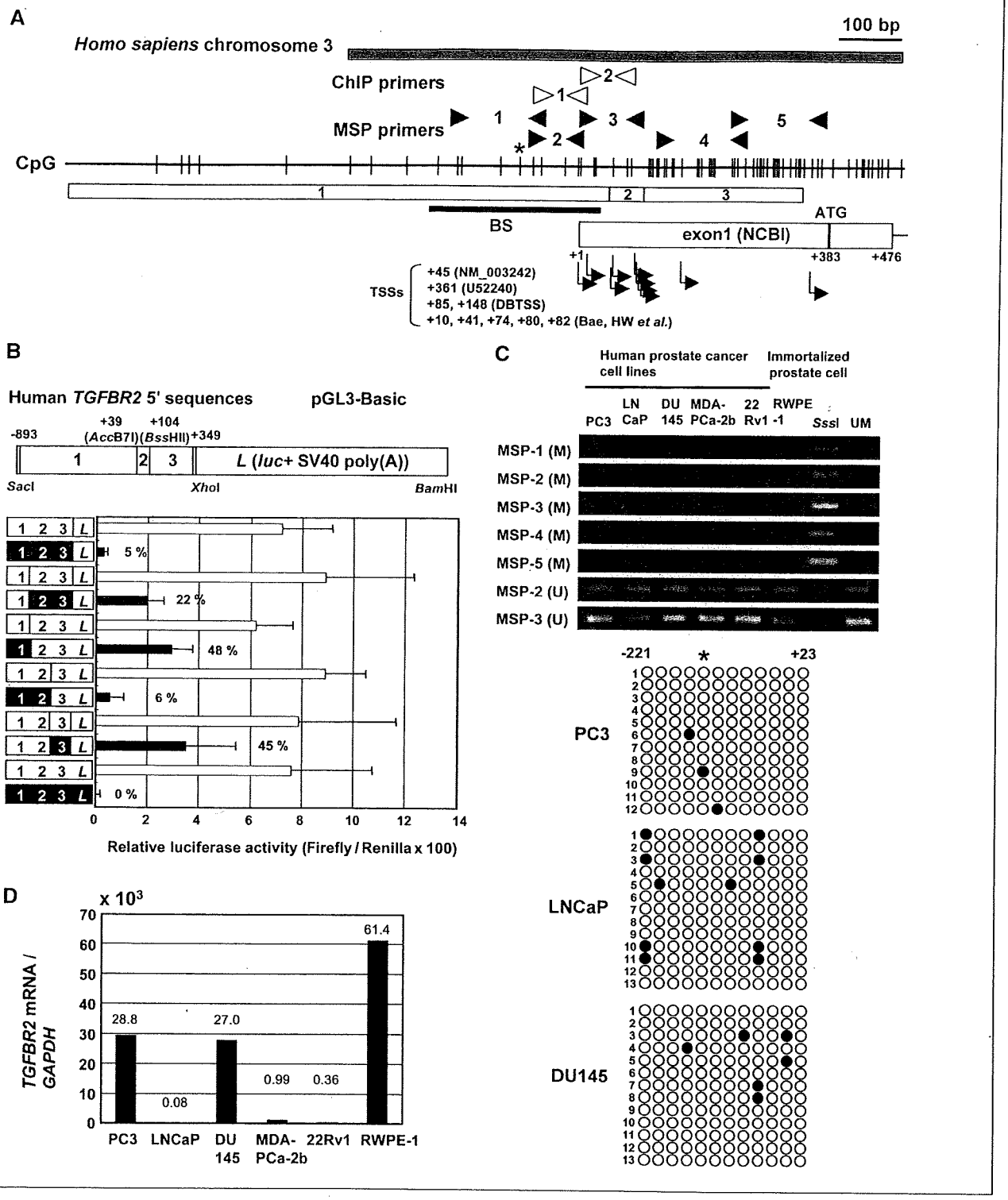

Figure 3. Human *TGFBR2* silencing due to dense methylation of its CGI, and its rare occurrence among human cancer cell lines. *A*, map of the promoter region and a CGI overlapping human *TGFBR2*. *+1*, TSS from the National Center for Biotechnology Information database (NC_000003.10, 30622998). Multiple TSSs reported (30) are also shown. *, a specific CpG site at nucleotide −140 (nucleotide −96 in this article) reported in ref. 36. *B*, structure of the *SacI-BamHI* DNA fragment used for the luciferase reporter assay (*top*). A DNA fragment spanning from −893 to +349 of human *TGFBR2* was ligated to the luciferase reporter gene. *Bottom*, luciferase activity of the reporter constructs with and without methylation of specific regions of the *TGFBR2* promoter. *Open* and *closed boxes*, unmethylated and methylated regions, respectively. The promoter activities were normalized to the activity of the cotransfected phRL-TK vector. Compared with the control without methylation, a reporter construct with methylation of regions 1 and 2 showed a marked decrease in luciferase activity. A fragment that had methylation of the entire reporter plasmid showed no transcription activity. *Columns*, mean; *bars*, SD. *C*, MSP of *TGFBR2* in five human prostate cancer cell lines and immortalized prostate epithelial cells (*RWPE-1*). Screening of 33 human cancer cell lines in the same manner showed that *TGFBR2* methylation was rare. *D*, real-time reverse transcription-PCR analysis of *TGFBR2* mRNA expression in human prostate cancer cell lines and RWPE-1. The expression was down-regulated to $<10^{-4}$ of that of *GAPDH* in LNCaP and to $<10^{-3}$ in MDA-PCa-2b and 22Rv1.

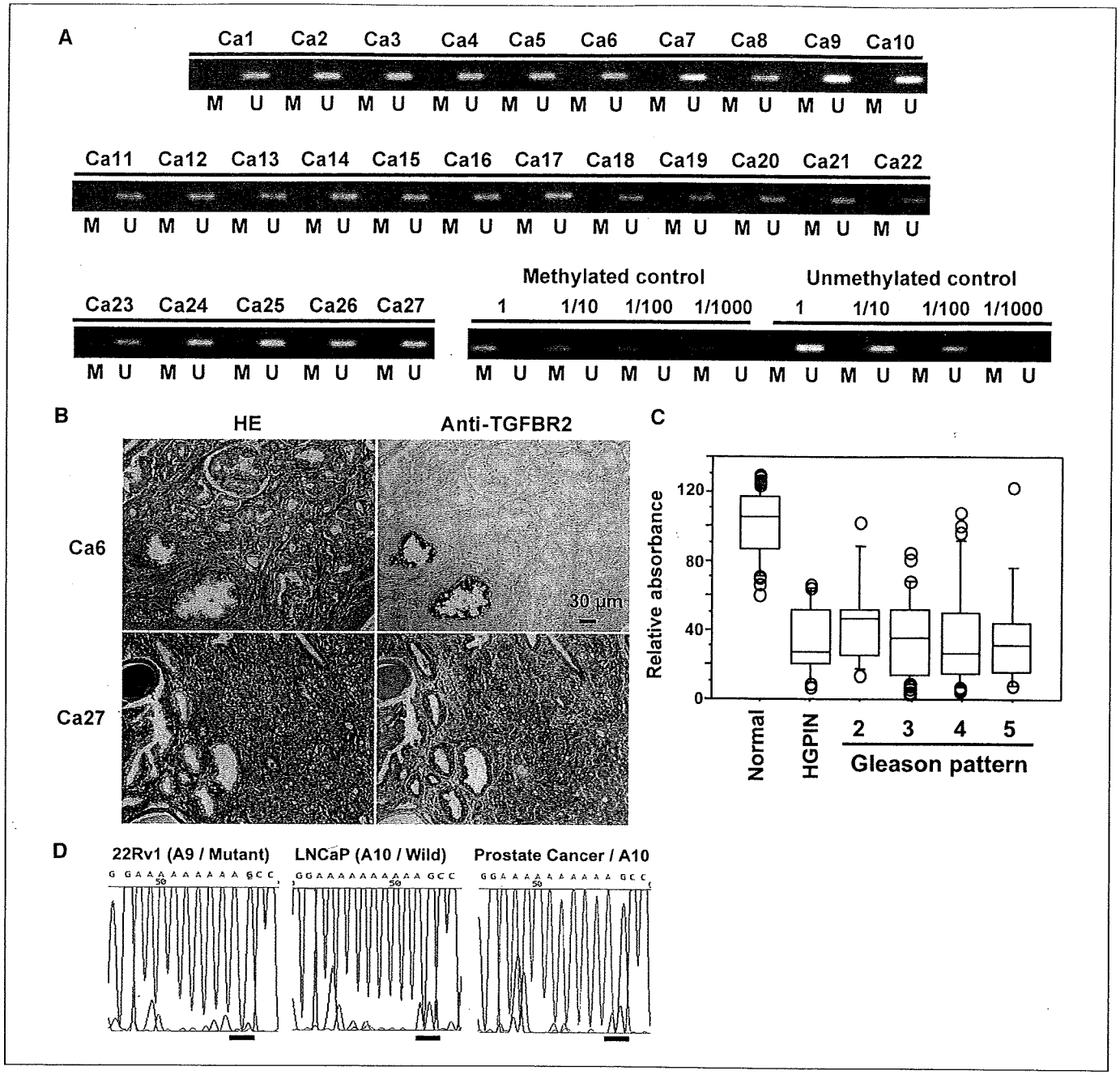

Figure 4. Absence of *TGFBR2* methylation and decreased TGFBR2 protein expression in primary human prostate cancers. *A*, methylation analysis of 27 primary human prostate cancers by MSP (MSP-3). PCR conditions were adjusted to allow detection of methylation of DNA molecules to as little as 1% of the positive control, but methylation was not detected. *B*, representative results of immunohistochemistry using anti-TGFBR2 antibody. *Ca6*, a cancer with decreased expression (*top*); *Ca27*, a cancer with positive expression (*bottom*). Decreased immunoreactivity was observed in 36 of 60 cases. *C*, TGFBR2 expression levels in HGPIN and prostate cancers with different Gleason patterns. Decreased TGFBR2 expression was already detected in HGPIN. *D*, representative results of mutation analysis. A10 (normal sequence) was deleted to A9 only in 22Rv1 and MDA-PCa-2b cell lines, and none of the 27 primary prostate cancers had a mutation.

the microarray was confirmed by quantitative reverse transcription-PCR (Supplementary Table S5). These eight genes were considered to be methylation-silenced in the rat prostate cancer cell lines.

Methylation silencing of *Tgfbr2* in rat prostate cancer cell lines. Interestingly, among the eight genes, *Tgfbr2*, a key mediator of TGF-β signaling that has been implicated in human and rat prostate carcinogenesis (12–19), was present. The methylation silencing of *Tgfbr2* was analyzed further. Generally, for methylation silencing, a dense DNA methylation of a region within a promoter CGI, specifically a region devoid of nucleosome just upstream of a transcription start site (TSS; nucleosome-devoid region), is critical (26, 27). To search for any *Tgfbr2* TSSs additional to the one reported in osteoblasts (28), we performed the 5′ RACE method using rat prostate cancer cell lines. Several TSSs were found to be located from +13 to +173 of the reported *Tgfbr2* TSS (NM_031132.3, National Center for Biotechnology Information; Fig. 1*A*), and the region analyzed by MSP was located at −178 to −22 of the multiple TSSs. Because this region

corresponded to the critical region involved in transcription repression, the presence of dense methylation was confirmed by bisulfite sequencing. PLS20 and PLS30 had only methylated DNA molecules, and PLS10 had both methylated and unmethylated DNA molecules before the 5-aza-dC treatment (Fig. 1*B*), consistent with the results by MSP (Fig. 1*C*).

The absence of *Tgfbr2* expression before the 5-aza-dC treatment and its re-expression after the treatment were confirmed by

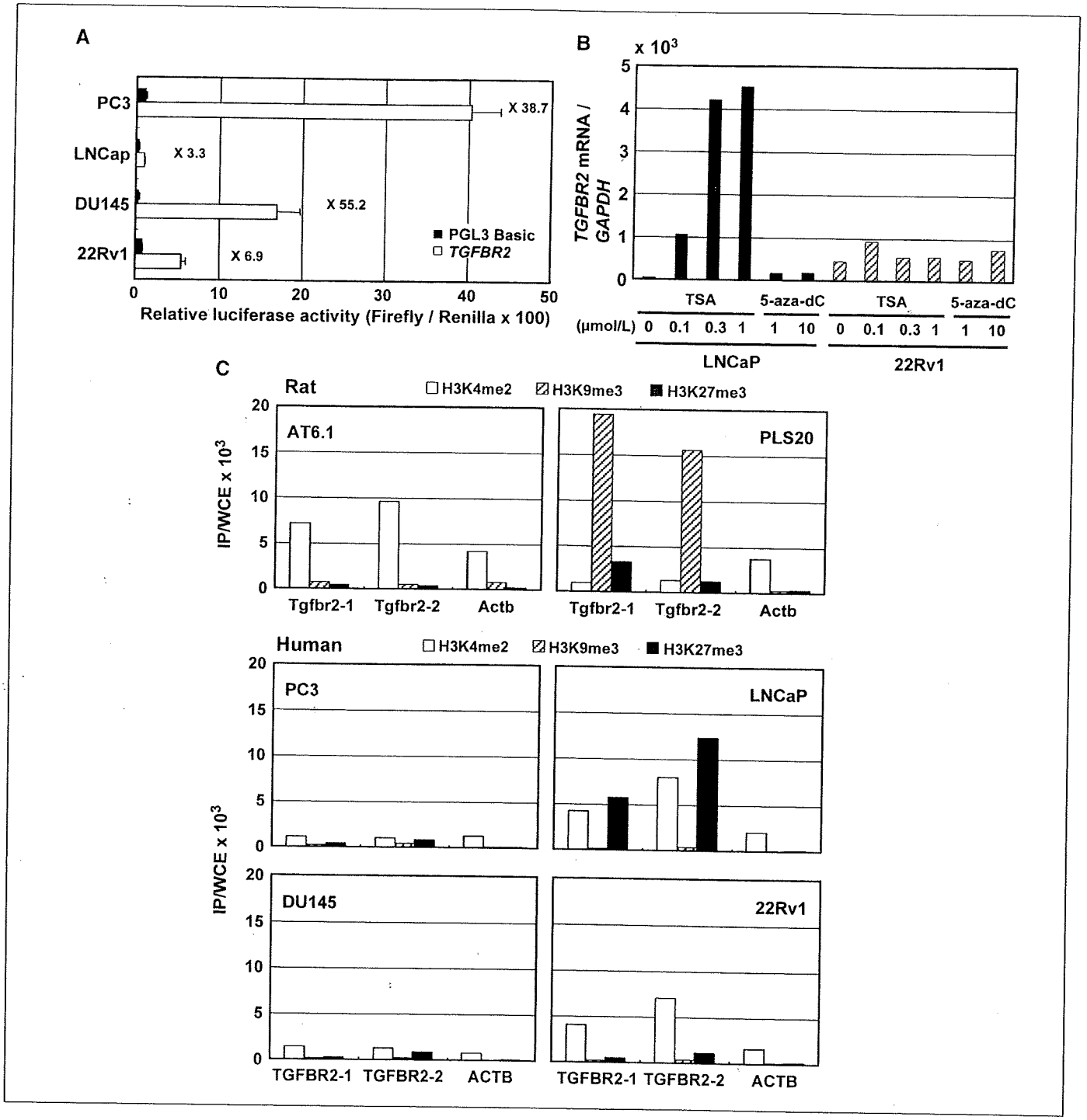

Figure 5. Transcriptional capacities and histone modifications of the *Tgfbr2* (*TGFBR2*) promoter in rat and human prostate cancer cell lines. *A*, luciferase reporter assay using a 1,242 bp DNA fragment covering the human *TGFBR2* promoter and TSSs. The DNA fragment had a 38.7-fold, 3.3-fold, 55.2-fold, and 6.9-fold higher luciferase activity in PC3, LNCaP, DU145 and 22Rv1, respectively, compared with control (pGL3-Basic vector without an inserted promoter DNA fragment). *B*, real-time reverse transcription-PCR analysis of *TGFBR2* mRNA expression in LNCaP and 22Rv1 cells with TSA or 5-aza-dC treatment. *C*, ChIP analysis of histone modifications at the *TGFBR2* and *ACTB* promoters in rat and human prostate cancer cell lines. At the *ACTB* promoter, increased H3K4me2 was observed in all rat and human prostate cancer cell lines. At the *Tgfbr2* promoter, a rat cell line with *Tgfbr2* expression (*AT6.1*) had increased H3K4me2 whereas another rat cell line without (*PLS20*) had increased H3K9me3. In contrast, human prostate cancer cell lines had both H3K4me2 and H3K27me3. Especially, a cell line with decreased *TGFBR2* expression (*LNCaP*) had H3K27me3. *IP*, immunoprecipitated; *WCE*, whole cell extract (input).

quantitative reverse transcription-PCR in PLS20 and PLS30 cells (Fig. 1*D*). The re-expression was associated with the appearance of unmethylated DNA molecules by MSP (Fig. 1*C*). Expression of *Tgfbr2* in the normal prostate, which is important for functional gene silencing in cancer, was confirmed. We concluded that *Tgfbr2* was methylation-silenced in PLS20 and PLS30 rat prostate cancer cell lines.

***Tgfbr2* silencing in rat primary prostate cancers.** DNA methylation of the *Tgfbr2* promoter CGI and its decreased protein expression were analyzed in rat primary prostate cancers induced by DMAB and testosterone. Using MSP, methylation was detected in three of seven invasive adenocarcinomas in the dorsolateral lobe, but in none of five noninvasive adenocarcinomas in the ventral lobe (Fig. 2*A*). Using immunohistochemistry, protein expression was found to be markedly decreased in the three invasive adenocarcinomas with methylation, but was not decreased in the remaining four invasive adenocarcinomas or in any of the five noninvasive adenocarcinomas (Fig. 2*B*). The results obtained by MSP were confirmed by bisulfite sequencing of two representative samples with and without methylation (Fig. 2*C*). These data showed that the *Tgfbr2* gene was methylation-silenced in rat primary prostate cancers induced by DMAB and testosterone.

Methylation silencing of human *TGFBR2*, and its rare occurrence. In humans, silencing of *TGFBR2* due to dense DNA methylation of its promoter CGI has been reported in a limited number of cell lines (29), but has not been found in any primary cancers. Unlike that of rat *Tgfbr2*, the "promoter CGI" of human *TGFBR2* is located mainly in its first exon, based on its well-documented multiple TSSs (Fig. 3*A*; ref. 30), and CpG density becomes lower in the promoter region. It is now known that DNA methylation of a nucleosome-devoid region is critical for gene silencing (26, 27), and that methylation of a promoter region with intermediate or low CpG density does not necessarily repress the transcription of its downstream gene (31). Therefore, we decided to examine whether or not dense methylation of various regions of human *TGFBR2* could cause its silencing.

First, a 1,242 bp DNA fragment covering the human *TGFBR2* TSSs and its promoter region was cloned. Then, the entire fragment or three regions (regions 1, 2, and 3; shown in Fig. 3*A* and *B*) and their combinations were specifically methylated, and the effect was analyzed by a reporter assay. Methylation of region 1 only (−893 to +39) and methylation of region 3 only (+104 to +349) reduced the promoter activity to half of their unmethylated controls (Fig. 3*B*). On the other hand, methylation of regions 1 and 2 (−893 to +104) reduced the activity to 6% of its unmethylated control. These data showed that dense methylation of the human *TGFBR2* CGI, if present, can repress transcription, and indicated that methylation of region 2 is indispensable. Due to the short size of region 2, data on methylation of region 2 only could not be prepared.

MSP primers were designed in region 2 (MSP-3), the possible nucleosome-devoid region, encompassing most TSSs, and methylation status was screened in 33 human cancer cell lines (five prostate, six ovarian, six lung, seven pancreatic, and nine stomach cancer cell lines; data for prostate cancers in Fig. 3*C*). Only TYK-nu (ovarian) and MIAPaCa-2 (pancreas) had *TGFBR2* methylation (data not shown). The lack of methylation in three prostate cancer cell lines (PC3, LNCaP, and DU145) was confirmed by bisulfite sequencing (Fig. 3*C*). When *TGFBR2* mRNA expression was examined, it was down-regulated to $<10^{-4}$ of that of *GAPDH* in LNCaP and to $<10^{-3}$ in MDA-PCa-2b and 22Rv1 (Fig. 3*D*). These data showed that silencing of *TGFBR2* due to dense methylation of its promoter region was rare among human cancer cell lines and absent in the five human prostate cancer cell lines analyzed.

Lack of methylation of the *TGFBR2* nucleosome-devoid region, but its frequent down-regulation in primary human prostate cancers. Methylation of the possible nucleosome-devoid region (MSP-3) was analyzed in 27 primary human prostate cancers by MSP. However, none of them showed methylation (Fig. 4*A*). It has been reported that TGFBR2 expression is markedly down-regulated in human prostate cancers (14–16), and we confirmed this. Following immunohistochemical analysis of the 20 high-grade prostatic intraepithelial neoplasia (HGPIN), the 27 cancers, and an additional 33 cancers, down-regulation of TGFBR2 protein was observed in 12 of 20 HGPIN and 36 of 60 prostate cancers (Fig. 4*B* and *C*). There was no correlation between expression levels of TGFBR2 protein and histologic grade in human prostate cancers. Finally, as a possible mechanism for decreased TGFBR2 expression, its mutations were searched for. Mutations were only detected in two prostate cancer cell lines (22Rv1 and MDA-PCa-2b), but not in the 27 primary prostate cancers analyzed (Fig. 4*D*).

Contrastive histone modifications in the rat and human prostate cancer cell line with down-regulated *Tgfbr2* expression. To analyze the molecular mechanisms causing down-regulation of *TGFBR2* in human prostate cancer cell lines (LNCaP and 22Rv1), we first analyzed their transcriptional capacity by a luciferase reporter assay using a 1,242 bp DNA fragment covering the human *TGFBR2* promoter and TSSs. The transcriptional capacity of LNCaP and 22Rv1 was significantly lower than that of PC3 and DU145 (Fig. 5*A*), although precise comparison of transcription activities among different cell lines was difficult because transfection and/or luminescence efficiencies were highly variable (Supplementary Table S6). We also analyzed the histone acetylation status in rat and prostate cancer cell lines by observing the effect of 5-aza-dC or TSA, a histone deacetylase inhibitor. LNCaP showed marked re-expression of *TGFBR2* mRNA after TSA treatment whereas 22Rv1 did not (Fig. 5*B*). This showed that, in addition to decreased transcription capacity, histone deacetylation was involved in the decreased *TGFBR2* expression in LNCaP, but not in 22Rv1.

Histone methylation status was further analyzed by chromatin immunoprecipitation (ChIP) assays in the rat and human prostate cancer cell lines. A rat cell line with *Tgfbr2* methylation silencing (PLS20) had increased H3K9me3, a typical mark for inactive chromatin (32), whereas another rat cell line with *Tgfbr2* expression (AT6.1) had increased H3K4me2, a typical mark for active chromatin (ref. 32; Fig. 5*C*). In contrast, human prostate cancer cell lines had both H3K4me2 and H3K27me3, and LNCaP, which had histone deacetylation, had a marked increase of H3K27me3 (Fig. 5*C*). These suggested that the loss of *Tgfbr2* expression in a rat prostate cancer cell line (PLS20) was due to DNA methylation, accompanied by the H3K9me3 modification, and that the decreased *TGFBR2* expression in a human prostate cancer cell line was due to decreased transcriptional capacity in concert with (LNCaP) or without (22Rv1) histone deacetylation and H3K27 trimethylation.

Discussion

Silencing of *Tgfbr2* was identified in invasive adenocarcinomas of the dorsolateral lobe of the rat prostate. This is the first report

of *Tgfbr2* silencing in animal cancers of any tissue, and of gene silencing in rat prostate cancers. In animal models, only a limited number of genes are known to be silenced by dense methylation of a region just upstream of a TSS, within a CGI, a nucleosome-devoid region (26, 27), in skin, lung, hematologic, and renal cancers (4–7). Our finding of *Tgfbr2* silencing in prostate cancers will enable us to analyze the processes of how aberrant methylation is induced *in vivo* and the factors that promote and suppress the induction of aberrant methylation, including testosterone. Mouse prostate cancers induced by the SV40 polyoma virus early region are known to be prevented by a demethylating agent, 5-aza-dC (33), but the genes responsible are still indefinite.

Functional involvement of *Tgfbr2* (TGFBR2) down-regulation in rodent and human prostate carcinogenesis is strongly supported in the literature. In rats, loss of TGF-β responsiveness in prostate epithelial cells causes malignant transformation (18), and prostate cancer sublines with high metastatic potential, MAT-LyLu and AT-3, show loss of Tgfbr2 protein (19). In mice, dominant negative Tgfbr2 mutant expression increased metastasis in the prostate of the TRAMP model (34), and conditional inactivation of *Tgfbr2* in fibroblasts resulted in intraepithelial neoplasia in the mouse prostate (35). In human prostate cancers, impaired TGF-β signaling, for which TGFBR2 is a key mediator, is likely to be deeply involved (12). Factors supporting this include, first, that TGF-β functions as an inducer of apoptosis in the normal prostate (12, 13); second, *TGFBR2* expression is reduced or lost in prostate cancers (14–16), as confirmed in this study; and third, overexpression of *TGFBR2* restores sensitivity of prostate cancer cells to apoptosis (12, 17). All these strongly indicate that *Tgfbr2* silencing is causally involved in rat prostate carcinogenesis, and suggest that *TGFBR2* down-regulation could be causally involved in human prostate carcinogenesis.

Human *TGFBR2* silencing due to dense methylation of its promoter region was first reported in lung cancer cell lines (29). Here, we showed that a critical region for its silencing was located just upstream of the human *TGFBR2* multiple TSSs (region 2, MSP-3), and that dense methylation of the region can repress its transcription. However, in human primary prostate cancers, *TGFBR2* silencing by dense methylation was not detected. The initial report on human *TGFBR2* silencing did not analyze primary cancers (29). These findings suggest that *TGFBR2* methylation silencing is very rare in human primary cancers. Methylation of a specific CpG site at −96 (nucleotide −140 in the original report) was reported to correlate with reduced *TGFBR2* expression in prostate cancer cell lines (36). However, we were not able to observe the correlation between methylation of the specific CpG site and transcription, or to detect dense methylation in any regions around the TSSs (MSP primers 1–5; Fig. 3*A* and *C*).

The rare occurrence of *TGFBR2* methylation silencing in human primary cancers was in sharp contrast with the frequent occurrence of *Tgfbr2* methylation silencing in rat invasive prostate cancers. Methylation silencing of genes other than *TGFBR2* are frequently observed in human prostate cancers (37). As a mechanism for the decreased *TGFBR2* expression, we first looked for *TGFBR2* mutations, but could not observe any. Then we analyzed transcriptional capacity and histone modifications, and revealed the presence of contrastive mechanisms between rats and humans. In the rat prostate cancer cell lines with *Tgfbr2* methylation silencing (PLS20 and PLS30), *Tgfbr2* expression levels were almost zero (Fig. 1*D*), their promoter regions were densely methylated, and had histone modification (H3K9me3) typical for inactive chromatin. In contrast, the human prostate cancer cell lines with decreased *TGFBR2* expression (LNCaP and 22Rv1) had very low levels of expression (Fig. 5*B*), decreased transcriptional capacity, and histone deacetylation and H3K27 trimethylation (LNCaP). The relative location of a CGI against the TSSs was markedly different between human and rat sequences, the human CGI mainly in exon 1 and the rat CGI mainly in the promoter region, and could be responsible for the contrastive mechanisms for the decreased *Tgfbr2* (*TGFBR2*) expression.

The induction mechanism of rat *Tgfbr2* silencing in the prostate is an interesting issue. Androgen exposure, a critical promoting factor of prostate cancers, is known to down-regulate *Tgfbr2* expression at the transcriptional level (38, 39), and transcriptional repression is known to trigger aberrant DNA methylation (3). In the rat prostate cancer model used here, a combination of an androgen (testosterone) and DMAB is important in inducing invasive prostate cancers, and thus *Tgfbr2* silencing. This suggests that not only the reduced *Tgfbr2* transcription but also some abnormality, required for induction of *Tgfbr2* silencing, is induced by testosterone and DMAB.

As for other methylation-silenced genes in the PLS rat prostate cancer cell lines, *Aebp1* is a binding partner for tumor-suppressor PTEN (40). *Gas6* and *Ocm* have oncogenic functions (41, 42). *Nnat* is known as an imprinting gene and its aberrant hypermethylation occurs frequently in pediatric acute leukemia (43). There is a possibility that silencing of these genes is related to the development and progression of rat prostate carcinoma. In human prostate cancers, two studies reported genomic screening of methylation-silenced genes (44, 45). No common genes were present between the genes identified in the two studies and the eight genes identified here. However, if we adopted a more relaxed criterion for screening of up-regulated genes in this study, *Tgfb3* (11-fold up-regulation in PLS10) was commonly identified (45). *Tgfb3* is also involved in TGF-β signaling, and is a candidate for a gene commonly methylation-silenced in both rat and human prostate cancers. Considering the number of methylation-silenced genes, it is likely that the majority of the genes silenced in PLS cells do not have causal roles in carcinogenesis.

In summary, we found *Tgfbr2* silencing due to dense DNA methylation of its promoter CGI in rat prostate cancers. This will enable us to analyze mechanisms of how methylation silencing is induced *in vivo* and identify factors that affect its induction.

Acknowledgments

Received 9/12/2007; revised 12/31/2007; accepted 1/18/2008.

Grant support: Grant-in-Aid for the Third-term Cancer Control Strategy Program from the Ministry of Health, Labour and Welfare, Japan. S. Yamashita is a recipient of a travel award from the Sankyo Foundation of Life Science, and N. McDonell is a recipient of a Foreign Scientist Fellowship from the Foundation for Promotion of Cancer Research.

The costs of publication of this article were defrayed in part by the payment of page charges. This article must therefore be hereby marked *advertisement* in accordance with 18 U.S.C. Section 1734 solely to indicate this fact.

We thank Dr. Yutaka Kondo, Aichi Cancer Center Research Institute, for his helpful advice in ChIP assays.

References

1. Jones PA, Baylin SB. The epigenomics of cancer. Cell 2007;128:683–92.
2. Ushijima T. Detection and interpretation of altered methylation patterns in cancer cells. Nat Rev Cancer 2005;5:223–31.
3. Ushijima T, Okochi-Takada E. Aberrant methylations in cancer cells: where do they come from? Cancer Sci 2005;96:206–11.
4. Fraga MF, Herranz M, Espada J, et al. A mouse skin multistage carcinogenesis model reflects the aberrant DNA methylation patterns of human tumors. Cancer Res 2004;64:5527–34.
5. Pulling LC, Vuillemenot BR, Hutt JA, Devereux TR, Belinsky SA. Aberrant promoter hypermethylation of the death-associated protein kinase gene is early and frequent in murine lung tumors induced by cigarette smoke and tobacco carcinogens. Cancer Res 2004;64:3844–8.
6. Yu L, Liu C, Vandeusen J, et al. Global assessment of promoter methylation in a mouse model of cancer identifies ID4 as a putative tumor-suppressor gene in human leukemia. Nat Genet 2005;37:265–74.
7. Dutta KK, Nishinaka Y, Masutani H, et al. Two distinct mechanisms for loss of thioredoxin-binding protein-2 in oxidative stress-induced renal carcinogenesis. Lab Invest 2005;85:798–807.
8. Parkin DM, Bray F, Ferlay J, Pisani P. Global cancer statistics, 2002. CA Cancer J Clin 2005;55:74–108.
9. Shirai T, Takahashi S, Cui L, et al. Experimental prostate carcinogenesis—rodent models. Mutat Res 2000;462:219–26.
10. Shirai T, Tamano S, Kato T, Iwasaki S, Takahashi S, Ito N. Induction of invasive carcinomas in the accessory sex organs other than the ventral prostate of rats given 3,2′-dimethyl-4-aminobiphenyl and testosterone propionate. Cancer Res 1991;51:1264–9.
11. Nakanishi H, Takeuchi S, Kato K, et al. Establishment and characterization of three androgen-independent, metastatic carcinoma cell lines from 3,2′-dimethyl-4-aminobiphenyl-induced prostatic tumors in F344 rats. Jpn J Cancer Res 1996;87:1218–26.
12. Danielpour D. Functions and regulation of transforming growth factor-β (TGF-β) in the prostate. Eur J Cancer 2005;41:846–57.
13. Martikainen P, Kyprianou N, Isaacs JT. Effect of transforming growth factor-β1 on proliferation and death of rat prostatic cells. Endocrinology 1990;127:2963–8.
14. Williams RH, Stapleton AM, Yang G, et al. Reduced levels of transforming growth factor β receptor type II in human prostate cancer: an immunohistochemical study. Clin Cancer Res 1996;2:635–40.
15. Kim IY, Ahn HJ, Zelner DJ, et al. Loss of expression of transforming growth factor β type I and type II receptors correlates with tumor grade in human prostate cancer tissues. Clin Cancer Res 1996;2:1255–61.
16. Guo Y, Jacobs SC, Kyprianou N. Down-regulation of protein and mRNA expression for transforming growth factor-β (TGF-β1) type I and type II receptors in human prostate cancer. Int J Cancer 1997;71:573–9.
17. Guo Y, Kyprianou N. Restoration of transforming growth factor β signaling pathway in human prostate cancer cells suppresses tumorigenicity via induction of caspase-1-mediated apoptosis. Cancer Res 1999;59:1366–71.
18. Tang B, de Castro K, Barnes HE, et al. Loss of responsiveness to transforming growth factor β induces malignant transformation of nontumorigenic rat prostate epithelial cells. Cancer Res 1999;59:4834–42.
19. Wikstrom P, Lindh G, Bergh A, Damber JE. Alterations of transforming growth factor β1 (TGF-β1) and TGFβ receptor expressions with progression in Dunning rat prostatic adenocarcinoma sublines. Urol Res 1999;27:185–93.
20. Shi SR, Cote RJ, Wu L, et al. DNA extraction from archival formalin-fixed, paraffin-embedded tissue sections based on the antigen retrieval principle: heating under the influence of pH. J Histochem Cytochem 2002;50:1005–11.
21. Yamashita S, Tsujino Y, Moriguchi K, Tatematsu M, Ushijima T. Chemical genomic screening for methylation-silenced genes in gastric cancer cell lines using 5-aza-2′-deoxycytidine treatment and oligonucleotide microarray. Cancer Sci 2006;97:64–71.
22. Moriguchi K, Yamashita S, Tsujino Y, Tatematsu M, Ushijima T. Larger numbers of silenced genes in cancer cell lines with increased *de novo* methylation of scattered CpG sites. Cancer Lett 2007;249:178–87.
23. Niwa T, Yamashita S, Tsukamoto T, et al. Whole-genome analyses of loss of heterozygosity and methylation analysis of four tumor-suppressor genes in *N*-methyl-*N*′-nitro-*N*-nitrosoguanidine-induced rat stomach carcinomas. Cancer Sci 2005;96:409–13.
24. Weisinger G, Gavish M, Mazurika C, Zinder O. Transcription of actin, cyclophilin and glyceraldehyde phosphate dehydrogenase genes: tissue- and treatment-specificity. Biochim Biophys Acta 1999;1446:225–32.
25. Markowitz S, Wang J, Myeroff L, et al. Inactivation of the type II TGF-β receptor in colon cancer cells with microsatellite instability. Science 1995;268:1336–8.
26. Lee CK, Shibata Y, Rao B, Strahl BD, Lieb JD. Evidence for nucleosome depletion at active regulatory regions genome-wide. Nat Genet 2004;36:900–5.
27. Fatemi M, Pao MM, Jeong S, et al. Footprinting of mammalian promoters: use of a CpG DNA methyltransferase revealing nucleosome positions at a single molecule level. Nucleic Acids Res 2005;33:e176.
28. Chang W, Parra M, Ji C, et al. Transcriptional and post-transcriptional regulation of transforming growth factor β type II receptor expression in osteoblasts. Gene 2002;299:65–77.
29. Osada H, Tatematsu Y, Masuda A, et al. Heterogeneous transforming growth factor (TGF)-β unresponsiveness and loss of TGF-β receptor type II expression caused by histone deacetylation in lung cancer cell lines. Cancer Res 2001;61:8331–9.
30. Bae HW, Geiser AG, Kim DH, et al. Characterization of the promoter region of the human transforming growth factor-β type II receptor gene. J Biol Chem 1995;270:29460–8.
31. Weber M, Hellmann I, Stadler MB, et al. Distribution, silencing potential and evolutionary impact of promoter DNA methylation in the human genome. Nat Genet 2007;39:457–66.
32. Li B, Carey M, Workman JL. The role of chromatin during transcription. Cell 2007;128:707–19.
33. McCabe MT, Low JA, Daignault S, Imperiale MJ, Wojno KJ, Day ML. Inhibition of DNA methyltransferase activity prevents tumorigenesis in a mouse model of prostate cancer. Cancer Res 2006;66:385–92.
34. Tu WH, Thomas TZ, Masumori N, et al. The loss of TGF-β signaling promotes prostate cancer metastasis. Neoplasia 2003;5:267–77.
35. Bhowmick NA, Chytil A, Plieth D, et al. TGF-β signaling in fibroblasts modulates the oncogenic potential of adjacent epithelia. Science 2004;303:848–51.
36. Zhao H, Shiina H, Greene KL, et al. CpG methylation at promoter site −140 inactivates TGFβ2 receptor gene in prostate cancer. Cancer 2005;104:44–52.
37. Dobosy JR, Roberts JL, Fu VX, Jarrard DF. The expanding role of epigenetics in the development, diagnosis and treatment of prostate cancer and benign prostatic hyperplasia. J Urol 2007;177:822–31.
38. Kim IY, Ahn HJ, Zelner DJ, Park L, Sensibar JA, Lee C. Expression and localization of transforming growth factor-β receptors type I and type II in the rat ventral prostate during regression. Mol Endocrinol 1996;10:107–15.
39. Nishi N, Oya H, Matsumoto K, Nakamura T, Miyanaka H, Wada F. Changes in gene expression of growth factors and their receptors during castration-induced involution and androgen-induced regrowth of rat prostates. Prostate 1996;28:139–52.
40. Gorbenko O, Kuznetsov V, Kukharenko O, et al. Identification of a novel binding partners for tumor suppressor PTEN by a yeast two-hybrid approach. Eksp Onkol 2004;26:15–9.
41. Sainaghi PP, Castello L, Bergamasco L, Galletti M, Bellosta P, Avanzi GC. Gas6 induces proliferation in prostate carcinoma cell lines expressing the Axl receptor. J Cell Physiol 2005;204:36–44.
42. Nestl A, Von Stein OD, Zatloukal K, et al. Gene expression patterns associated with the metastatic phenotype in rodent and human tumors. Cancer Res 2001;61:1569–77.
43. Kuerbitz SJ, Pahys J, Wilson A, Compitello N, Gray TA. Hypermethylation of the imprinted NNAT locus occurs frequently in pediatric acute leukemia. Carcinogenesis 2002;23:559–64.
44. Lodygin D, Epanchintsev A, Menssen A, Diebold J, Hermeking H. Functional epigenomics identifies genes frequently silenced in prostate cancer. Cancer Res 2005;65:4218–27.
45. Yu YP, Paranjpe S, Nelson J, et al. High throughput screening of methylation status of genes in prostate cancer using an oligonucleotide methylation array. Carcinogenesis 2005;26:471–9.

RESEARCH COMMUNICATION

Suppression of Prostate Cancer Growth by Resveratrol in The Transgenic Rat for Adenocarcinoma of Prostate (TRAP) Model

Azman Seeni, Satoru Takahashi*, Kentaro Takeshita, Mingxi Tang, Satoshi Sugiura, Shin-ya Sato, Tomoyuki Shirai

Abstract

Research into actions of resveratrol, abundantly present in red grape skin, has been greatly stimulated by its reported beneficial health influence. Since it was recently proposed as a potential prostate cancer chemopreventive agent, we here performed an in vivo experiment to explore its effect in the Transgenic Rat for Adenocarcinoma of Prostate (TRAP) model, featuring the rat probasin promoter/SV 40 T antigen. Resveratrol suppressed prostate cancer growth and induction of apoptosis through androgen receptor (AR) down-regulation, without any sign of toxicity. Resveratrol not only downregulated androgen receptor (AR) expression but also suppressed the androgen responsive glandular kallikrein 11 (Gk11), known to be an ortholog of the human prostate specific antigen (PSA), at the mRNA level. The data provide a mechanistic basis for resveratrol chemopreventive efficacy against prostate cancer.

Key Words: Chemoprevention - prostate cancer - resveratrol - TRAP rats

-Asian Pacific J Cancer Prev, 9, 7-14

Introduction

Prostate cancer has become the most frequently diagnosed cancer and the second leading cause of cancer-related death for men in the United States (Jemal et al., 2007). The conventional treatments available for this disease, such as hormone therapy, chemotherapy or radical prostatectomy, eventually fail to exert control and metastatic disease frequently develops even after surgery and may cause death. Therefore, interest has focused on chemoprevention, suppressing, delaying or reversing carcinogenesis by pharmacologic intervention with naturally occurring or synthetic agents (Sporn and Suh, 2002;Tsao et al., 2004).

Resveratrol, a phytoestrogen, found in grapes and red wine, has been identified as a novel potential cancer chemopreventive agent. Numerous reviews have been published regarding its activity (Jang et al., 1997;Bhat and Pezzuto, 2002; Stewart et al., 2003; Aziz et al., 2003; Aggarwal et al., 2004; Baur and Sinclair, 2006; Delmas et al., 2006) but the molecular mechanisms have yet to be fully defined, especially *in vivo*. Therefore, we explored the effects of resveratrol using the Transgenic Rat for Adenocarcinoma of Prostate (TRAP) model, established in our laboratory using the Simian virus 40 T antigen under control of the probasin gene promoter (Asamoto et al., 2001a; Asamoto et al., 2002). The animals develop high grade prostatic intraepithelial neoplasia (PIN) and well differentiated adenocarcinoma with high incidence in all prostate lobes at 15 weeks of age, all lesions being completely androgen-dependent. The model provides an ideal tool to gain insights into possible mechanisms for prostate cancer prevention (Asamoto et al., 2001b; Cho et al., 2003; Zeng et al., 2005; Kandori et al., 2005; Said et al., 2006; Tang et al., 2007) in the relatively short-term. To our knowledge, the present study provided the first evidence that resveratrol inhibits prostate carcinogenesis in a rat model closely mimicking the human disease. The clues obtained as to the molecular basis of action are of critical importance as the first steps towards human clinical trials.

Materials and Methods

Animals

Male heterozygous TRAP rats were housed three per plastic cage on wood-chip bedding in an air conditioned specific pathogen free (SPF) animal room under standard conditions with food (Oriental MF, Oriental Yeast, Tokyo, Japan) and water *ad libitum*. All animal experiments were performed under protocols approved by the Institutional Animal Care and Use Committee of Nagoya City University Graduate School of Medical Sciences.

Chemicals, reagents and cell lines

Resveratrol was purchased from Sigma, and MG132 and cycloheximide from Calbiochem (EMD Biosciences, Inc., San Diego, CA). Antibodies to cleaved caspase 3, 7, Erk1/2 and phospho-Erk1/2 were purchased from Cell Signaling Technology (Beverly, MA). Anti-AR antibody (PG-21) was from Upstate Technology (Lake Placid, NY), anti-HA-Tag antibody was from BD Sciences Clontech

*Department of Experimental Pathology and Tumor Biology, Nagoya City University Graduate School of Medical Sciences, Nagoya, 467-8601, Japan. *For Correspondence : E-mail: sattak@med.nagoya-cu.ac.jp FAX: +81-52-842-0817*

(Palo Alto, CA), anti-cyclin D1 was from Oncogene Research Product, anti-Bcl-xL was from Pharmingen, anti-SV40T Ag was from Santa Cruz Biotechnology Inc. and anti-β-actin was from Sigma. COS7 and LNCaP were from the American Type Culture Collection (Manassas, VA). PLS30 cells were established in our laboratory as described previously (Nakanishi et al., 1996; Kato et al., 1998).

Plasmids

To generate pBKCMV-rAR, the rat AR open reading frame (ORF) was amplified by PCR and inserted into pBKCMV (Stratagene). For pGL3-rPBP-luc, a rat probasin promoter fragment (-426 ~ +32) was amplified and inserted into pGL3-basic (Promega). HA-tagged ubiquitin (MT123) was a generous gift from Dr. Dirk Bohmann (University of Rochester Medical Center).

Experimental design

A total of 48 heterozygous transgenic male rats were divided into four equally sized groups. Beginning at the age of three weeks, rats of each group received resveratrol at the concentration of 50, 100 or 200 μg/ml or normal drinking water as the control. Body weights and water consumption were recorded weekly. At 10 weeks of age, all surviving rats were sacrificed and prostates were removed and weighed. Half of each ventral prostate was immediately frozen in liquid nitrogen for storage until processed. The remainder of each prostate was fixed in formalin and routinely processed for embedding in paraffin and sectioning for H&E staining and histopathological evaluation as well as immunohistochemistry. Testosterone and estradiol levels in serum were analysed by radioimmunoassay in a commercial laboratory (SRL, Tokyo, Japan).

Assessment of prostate neoplastic lesion development

Our TRAP rats showed sequential development of prostatic lesions, i.e. low- and high-grade prostatic intraepithelial neoplasias (PINs) to differentiated adenocarcinomas. Low-grade PIN (LG-PIN) were characterized by having with one or two layers of atypical cells with hyperchromatic nuclei and intact gland profiles and high-grade PIN (HG-PIN) showing increased epithelial stratification with nuclear atypia. Adenocarcinomas were characterized by atypical cells fill almost the lumen of the ducts with cribriform structures or solid growth in acini (Figure 1). The relative numbers of acini with the histological characteristics were quantified by counting for every features, e.g. LG-PIN, HG-PIN and adenocarcinoma, from the total acini in each prostatic lobe and calculated the percentages of each lesions by H&E staining and epithelial contents in acinic areas by performed Azan-Mallory histochemical staining to determine the progression of neoplastic lesions. Red staining areas in the prostates were equivalent to viable epithelial lesions and were quantitatively measured with an Image Processor for Analytical Pathology (IPAP, Sumika Technos Co., Osaka, Japan).

Immunohistochemistry

For Ki-67 immunostaining, deparaffinized sections were incubated with diluted rabbit polyclonal Ki-67 antibody (Novocastra). Apoptotic cells were detected using an In situ Apoptosis Detection Kit (TUNEL method) according to the manufacturer's instructions (Takara Bio Co. Ltd). Labeling indices were counted separately in the ventral, dorsal and lateral prostate and expressed as numbers of Ki-67-positive or TUNEL-positive cells per 100 cells.

Western blot analysis

Cells were lysed in RIPA buffer containing 150 mM NaCl, 1% NP-40, 0.5% sodium deoxycholate, 0.1% SDS, 50 mM Tris-HCl (pH8.0), 0.2 mM sodium orthovanadate and Complete Cocktail (Roche). Cell lysates were electrophoresed through SDS-PAGE gels and blotted onto nitrocellulose membranes. Immunoreactive protein bands were visualized using an ECL plus kit (Amersham Pharmacia Biotech, Freiburg, Germany).

Reverse Transcription-PCR and Real Time-RT PCR

Total RNA was isolated using an RNeasy Mini Kit (Qiagen). Total RNAs were reverse-transcribed with the SuperScript First-Strand Synthesis System (Invitrogen Life Technologies) and amplified by PCR (RT-PCR) using specific primers for AR and GAPDH. Primers used were

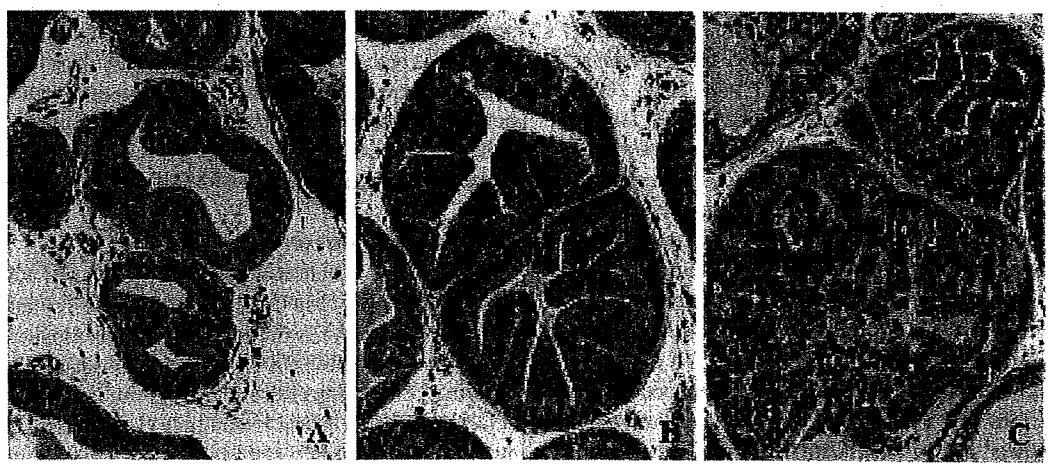

Figure 1. Representative Histopathological Findings for LG-PIN (A), HG-PIN (B) and Adenocarcinoma (C) in Ventral Prostates of TRAP Rats

as follows: (a) AR, forward primer 5-TTGTGAACAGAGTCCCCTAT-3, reverse primer 5-TTCTGGGATGGGTCCTCAGT-3, and (b) GAPDH, forward primer 5-GCGAGATCCCGTCAAGATCA-3, reverse primer 5-CCACAGTCTTCTGAGTGGCAG-3. Real-time quantitative RT-PCR was performed for androgen responsive gene, Gk11 expression using LightCycler (Roche Diagnostics). The primers used to detect GK11 genes are as follows: forward primer 5-GCAGCACCAAACCCCTGGAT-3, reverse primer 5-TGAGATCTGTCACCTTCTCA-3, and primers for rat cyclophilin (used as internal control) are as follows: forward primer 5-TGCTGGACCAAACACAAATG-3, reverse primer 5-GAAGGTGAAAGAAGGCATGA-3.

Reporter gene assay

COS7 cells were transfected with pBKCMV-rAR and pGL3-rPBP-luc using Nucleofector II (Amaxa, Germany). Twenty-four hours after transfection, 10 nM DHT and/or resveratrol was added for another 24 hrs. Cells were lysed with the buffer supplied in the kit 24 hr after transfection. The luciferase assay was conducted using the dual-luciferase reporter assay system (Promega), and the phRL-TK vector (Promega) was used as an internal control. Data shown represent the average and standard deviation of four independent data points.

AR stability assay

COS7 cells were transfected with pBKCMV-rAR, plated into 6-well plate and incubated for 24 hrs. Cells were pretreated with 10 μg/ml cycloheximide for 30 min and then were added 200 μM resveratrol or DMSO. Cells were lysed with RIPA buffer at 0, 1, 2, 4 and 8 hrs after adding resveratrol or DMSO, and cell lysates were subjected to western blot analysis.

Ubiquitylation assay

COS7 cells were transfected with pBKCMV-rAR and MT123 using Nucleofector II, plated into 6-well plates and incubated for 24 hrs. Cells were treated with resveratrol and/or 1 μM MG132 for 24 hrs, and then lysed with IP lysis buffer containing 20 mM Tris-HCl, pH7.5, 150 mM NaCl, 1 mM EDTA, 1 mM EGTA, 1% Triton X-100, 2.5 mM sodium pyrophosphate, 1 mM beta-glycerophosphate, 1 mM sodium orthovanadate, and Complete Cocktail. Immunoprecipitation was performed using rabbit anti-AR antibodies, and subjected to western blot analysis using anti-HA-Tag antibodies.

AR translation assay

COS7 cells were transfected with pBKCMV-rAR using Nucleofector II, seeded into 6-well plate and incubated for 24 hrs. Cells were pretreated with 100, 200 μM resveratrol or DMSO for 13 hrs, and medium was changed to methionine-, cysteine-free RPMI1640/10% FBS with or without resveratrol at 37°C for 1.5 hrs thereafter. Cells were incubated with methionine-, cysteine-free RPMI1640/10% FBS containing 100 μCi/ml Premix [^{35}S]methionine and [^{35}S]cysteine and unlabeled methionine and cysteine (5 μM each) for 1, 2, 4 and 8 hrs. Cold IP lysis buffer was added to each well to lyse cells. One hundred micrograms of cellular protein were immunoprecipitated with rabbit anti-AR antibodies, and samples were subjected to gel electrophoresis, followed by autoradiographic signal quantitation using NIH image software.

Metastasis assay in nude mice

PLS30 cells ($5x10^6$/animal) were injected into the subcutis of 6-week-old male athymic nude mice of the CD-1 strain (Charles River Japan, Inc, Kanagawa). One week after injection, mice were given resveratrol at concentrations of 100 and 200 μg/ml in their drinking water. Six weeks after injection, mice were sacrificed and examined for numbers of metastatic foci in lungs stained with Indian ink (Wexler, 1966).

Statistical analysis.

Data are expressed as means ± SDs. Differences in means between groups were determined by analysis of variance (ANOVA), followed by the Scheffe's post-hoc test with StatView (version 5.0) software (SAS Institute, Inc., Cary, NC). The Spearman's rank correlation coefficient test was used for analysis of dependent data.

Results

Body weight and water consumption

Resveratrol did not cause mortality or non-significant changes in body and relative organ weights (ventral prostate, liver and kidney) compared to the control group. The groups also did not differ in water consumption. Average resveratrol intake was consistent with the doses given, as shown in Table 1.

Testosterone and estradiol levels in serum

Although serum testosterone levels were significantly reduced in the 50 and 100 microgram/ml resveratrol treatment groups compared to control group values, unfortunately we found that the latter were higher than the normal range, which is about 1 - 2 ng/ml (Zeng et al., 2005; Kandori et al., 2005; Cho et al., 2003; Asamoto et al., 2002) (Table 1). Thus, the results were unexplainable regarding effects of resveratrol on serum testosterone. No

Table 1. Serum Testosterone, Estradiol Levels and the Average Resveratrol Intake of TRAP Rats

Treatment	No. of rats	Testosterone (ng/ml)	Estradiol (pg/ml)	Average resveratrol intake (mg/kg/day)
Control	12	4.28±3.15	4.75±1.11	-
Resveratrol 50 ug/ml	12	1.31±0.81*	4.46±1.47	7.59±1.15
Resveratrol 100 ug/ml	12	0.88±0.40*	3.91±0.99	16.11±2.42
Resveratrol 200 ug/ml	12	4.44±2.27	4.79±1.15	30.05±5.90

Data are means ± SD, *, P<0.01 versus control

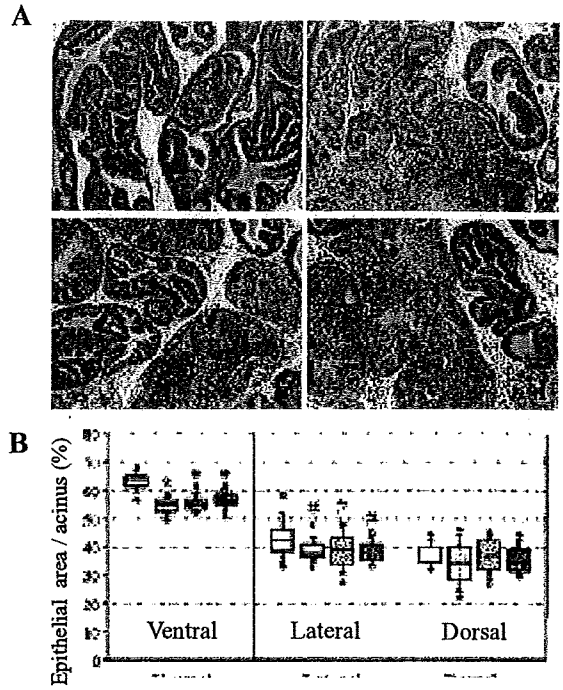

Figure 2. Effects of Resveratrol on Ventral Prostate Adenocarcinomas. (A) Representative histological appearances of (a) control and resveratrol (b) 50 (c) 100 and (d) 200 ug/ml (H &E staining). (B) Quantitative analysis of relative epithelial areas within prostatic acini of TRAP rats. Data are means ± SD for 12 animals. *, P < 0.01 versus control. #, P < 0.05 versus control (Spearman 's rank correlation coefficient test). Boxes left to right: Control; resveratrol 50;100; 200 ug/ml

significant changes were noted in serum estradiol levels compared to controls (Table 1).

Effects of resveratrol treatment on development of neoplastic lesions in the prostate

There were partial pathologic responses to resveratrol treatment as demonstrated by reduction in the content of prostatic neoplastic lesions in TRAP rats (Figure 2A). However, small foci of carcinoma remained, so that there were no significant differences in the incidences of PIN or adenocarcinoma in the prostates of TRAP rats (Table 2). There were no adenocarcinomas in the dorsal and anterior lobes in all groups of rat. As the entire ventral and lateral prostate lobes were occupied with tumor lesions and clear differences in prostate adenocarcinoma incidence were not observed among the groups, we evaluated the areas of epithelium including tumors morphometrically. The results, as summarized in Figure 2B, showed that resveratrol treatment significantly suppressed neoplastic lesion development about 14%, even at low dose (50 μg/ml) in the ventral lobes and also in the lateral lobes with a dose-dependent manner. Furthermore, evaluation of the proportion of preneoplastic and neoplastic lesions showed that resveratrol tended to shift the progression of neoplastic growth by suppressed the number of adenocarcinoma and HG-PIN and consequently, increased LG-PIN in all lobes (Table 3). The numbers of apoptotic cells in the ventral prostate of rats treated with resveratrol were also significantly increased as compared with the controls, while there were no obvious differences in Ki-67 labeling indices (Table 4).

Resveratrol downregulates AR and Gkl1 in the ventral prostate

Figure 3A shows that resveratrol clearly suppressed AR protein expression even at low dose of 50 μg/ml and also slightly suppressed SV40 Tag expression at the high dose. RT-PCR analysis of the AR gene showed no obvious differences at the AR mRNA level (Figure 3B), suggesting post-transcriptional downregulation. However, mRNA expression of the androgen responsive gene, Gk11, was significantly suppressed in the ventral prostate (Fig 3C).

Resveratrol affects AR function and its stability in vitro

In COS7 cells transfected with pBKCMV/rAR, resveratrol repressed exogenous AR expression, as well as endogenously in the LNCaP cells (Figure 4A). Subsequent reporter assays clearly demonstrated inhibition of functional AR activity in a dose-dependent manner, this being considered to simply reflect downregulation of AR protein expression by resveratrol. In resveratrol-treated cells, the half-life of AR protein was also slightly reduced, with a one hour difference compared to control cells (Figure 4B), suggesting an influence on AR protein degradation. The suppressive effect of resveratrol was not

Table 2. Incidences of Prostate Adenocarcinomas in TRAP Rats Treated with Resveratrol

Treatment	No. of rats	Incidence of adenocarcinoma (%)			
		Ventral	Lateral	Dorsal	Anterior
Control	12	11 (92)	4 (33)	0	0
Resveratrol 50 ug/ml	12	10 (83)	2 (17)	0	0
Resveratrol 100 ug/ml	12	10 (83)	5 (42)	0	0
Resveratrol 200 ug/ml	12	9 (75)	2 (17)	0	0

Table 3. Quantitative Evaluation of Neoplastic Lesions in Prostate of TRAP Rats Treated with Resveratrol

Treatment	No. of rats	Relative number of acini with histological characteristics(%)								
		Ventral			Lateral			Dorsal		
		LG-PIN	HG-PIN	Carcinoma	LG-PIN	HG-PIN	Carcinoma	LG-PIN	HG-PIN	Carcinoma
Control	12	3.1±1.0	95.3±1.0	1.6±0.5	20.7±12.0	77.6±11.4	1.7±1.6	24.4±10.8	75.6±10.8	-
Resveratrol 50 ug/ml	12	4.8±2.2*	93.9±1.9*	1.3±0.5#	23.5±11.3	75.8±11.0	0.6±0.6*	31.7±20.1	68.3±20.1	-
Resveratrol 100 ug/ml	12	3.7±1.4	95.1±1.5	1.2±0.4*#	18.7± 8.0	80.6± 7.7	0.6± 0.7	28.6±12.0	71.4±12.0	-
Resveratrol 200 ug/ml	12	4.0±1.5	94.9±1.4	1.1±0.4*#	22.9± 9.2	76.5± 9.3	0.6±0.9	30.7±16.7	69.3±16.7	-

Data are mean ± SD *, P<0.05 versus control #, P<0.05 versus control (Spearman's rank correlation coefficient test)

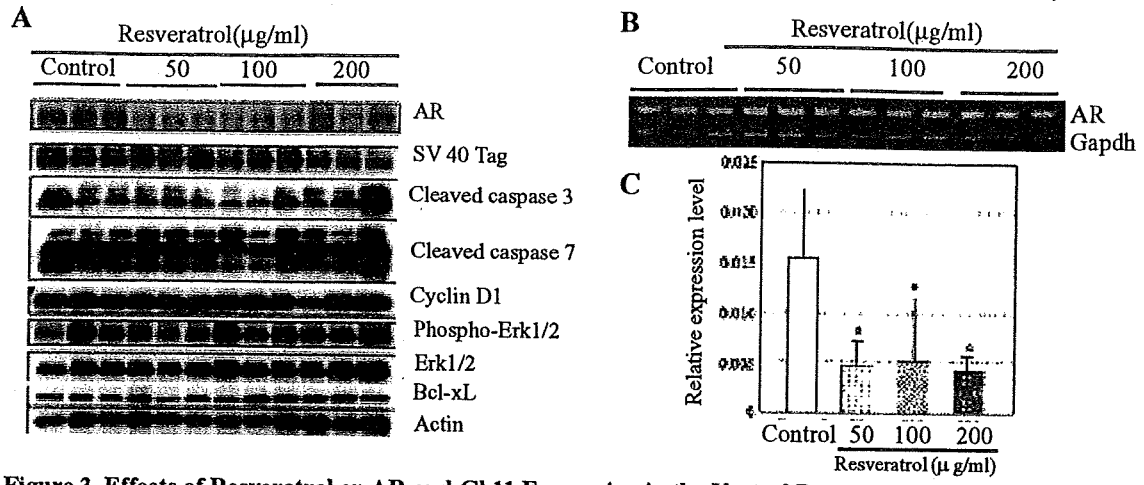

Figure 3. Effects of Resveratrol on AR and Gk11 Expression in the Ventral Prostates of TRAP rats. (A) Western blot analysis for AR, MAPK and apoptosis-related proteins; (B) RT-PCR analysis for AR; (C) Real Time-RT PCR analysis for Gk11 expression normalized to cyclophilin used as an internal control. Data are means ± SD of five animals. *, $P < 0.05$ versus control

completely blocked by the proteasome inhibitor, MG132 (Figure 4C), suggesting that resveratrol-induced AR protein down-regulation is not mainly via the proteasome-dependent pathway.

Resveratrol suppresses AR translation in vitro

To further determine the possible mechanism involved in the regulation of AR expression at the posttranscriptional level, AR-translation *in vitro* assay was performed to characterize whether resveratrol affects AR protein translation efficiency. Figure 4D shows that treatment with resveratrol reduced AR protein synthesis by about 40% as compared with untreated cells. This inhibitory phenomena might be specific on AR protein translation because resveratrol did not affected the translation of ERK1 and Cyclin D1, which been chosen as control protein, using LNCaP cells (data not shown).

Effects of resveratrol on lung metastasis in nude mice

There were no significant differences in growth of

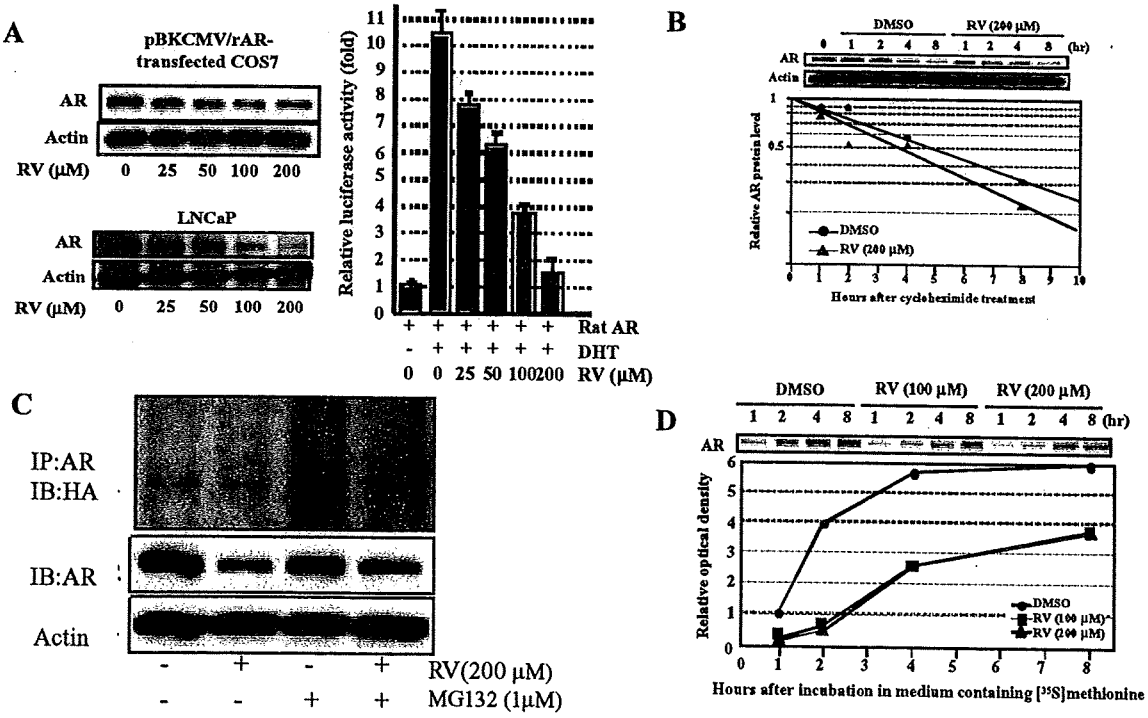

Figure 4. Mechanisms of Down-regulation of AR Protein by Resveratrol. (A) *Left panel*, western blot analysis of AR in transiently pBKCMV/rAR-transfected COS7 cells (top) and in LNCaP cells (*below*). *Right panel*, Reporter gene assay for AR. Means ± SD. (B) AR protein stability assay of COS7 cells transfected with pBKCMV/rAR, pretreated with cycloheximide and then treated with 200 uM resveratrol or DMSO. AR protein levels were determined by western blot analysis and normalized to actin (*top*). The AR expression was quantified and plotted relative to time 0. (C) Ubiquitylation assay for AR in COS7 cells transfected with both pBKCMV/rAR and pMT123 (HA-Ub), treated with resveratrol and/ or MG132. (D) AR translation assay of COS7 cells transfected with pBKCMV/rAR and incubated for 24 hrs. Details are described in the *Materials and Methods*

Table 4. Ki-67 Labeling index (%) and Apoptotic Indices in Prostate of TRAP Rats Treated with Resveratrol

Treatment	No. of rats	Ki-67 labeling			Apoptotic index (%)		
		Ventral	Lateral	Dorsal	Ventral	Lateral	Dorsal
Control	12	22.6±3.3	23.0±4.8	14.1±3.2	3.6±1.2	2.7±1.1	0.9±0.3
Resveratrol 50 ug/ml	12	23.7±6.0	23.3±6.0	14.8±3.7	5.5±1.9*	2.9±1.0	0.8±0.3
Resveratrol 100 ug/ml	12	22.0±4.4	22.1±3.9	15.1±3.9	5.4±1.9*	3.6± 1.8	0.9±0.3
Resveratrol 200 ug/ml	12	20.6±4.0	26.0±6.7	17.4±3.8	5.4±1.6*	2.4±1.2	0.8±0.2

Data are mean ± SD *, P<0.01 versus control

xenografts or lung metastases after subcutaneous injection of the PLS30 cell line into the flanks of athymic nude mice and treatment with resveratrol (Table 5).

Discussion

There was no report regarding the effectiveness of resveratrol in preclinical animal model of prostate cancer so far (Syed et al., 2007). The present study demonstrated, for the first time to our knowledge, suppressive effects of resveratrol on prostate cancer growth and induction of apoptosis through AR down-regulation in an *in vivo* rat model. This *in vivo* finding is an important step in verifying potential chemoprevention by resveratrol before recommending use in humans. Well-designed *in vivo* animal study plays a critical role between the *in vitro* experiment and clinical trials especially for the optimal dosing and toxicity of the agent. Importantly, the inhibition effect was achieved without any significant change in final body weights, relative liver and kidney weights and water consumption. Lack of signs of toxicity in the present experiment is in line with the earlier finding that oral intake of high dose (20 mg/kg/day) of resveratrol is not harmful to rats (Juan et al., 2002), although the dosage of resveratrol employed in this study was equivalent to 400 - 1,600 times the amount consumed by a person with ordinary wine intake (Gescher and Steward, 2003). The previous report showed that serum concentration of free, 3- and 4'-glucuronide of resveratrol in healthy human with moderate consumption of red wine were up to 26 nM, 190 nM and 2.2 uM, respectively (Vitaglione et al., 2005), and we used the dose of resveratrol that was equivalent to about 100 times concentration compared to these human data in *in vitro* study.

Resveratrol is well known for its phytoestrogenic and antioxidant properties (Baur and Sinclair, 2006) and exerts a variety of beneficial effects in humans, such as protection against the metabolic syndrome (Lagouge et al., 2006),

Table 5. In Vivo Growth and Lung Metastasis of PLS30 rat Prostate Cancer Cells in Nude Mice Treated with Resveratrol

Treatment	No. of mice	Tumor volume of xenograft(cm^3)	No. of metastatic foci in lungs
Control	11	0.96 ± 0.49	50.6 ± 38.9
Resveratrol 100 ug/ml	10	1.10 ± 0.47	35.0 ± 24.5
Resveratrol 200 ug/ml	10	0.85 ± 0.40	38.2 ± 28.5

Data are means ± SD

inflammation and viral infection (Friel and Lederman, 2006). Recently it was also shown to have a possible positive influence on life-expectancy, since food supplementation with resveratrol prolonged lifespan and retarded the expression of age-dependent traits in a short-lived vertebrate (Valenzano et al., 2006; Baur et al., 2006). A population-based case-control study further suggested that consumption of red wine may be associated with a reduction of the relative risk of prostate cancer (Schoonen et al., 2005) and resveratrol is probably one of the main microcomponents of wine responsible. The suppressive effect on AR expression by resveratrol in our study is agreement with earlier *in vitro* findings (Jones et al., 2005; Hsieh and Wu, 2000; Mitchell et al., 1999), as well as the hypothesis that resveratrol results in scavenging of incipient populations of androgen-dependent prostate cancer cells through its influence on the AR (Kyprianou and isaacs, 1988). *In vitro* studies have also indicated that resveratrol has marked antiandrogenic effects, in the androgen-dependent human prostate cell line LNCaP, that involve suppression of AR, the AR-specific co-activator ARA70 and various AR-regulated genes and that these effects are associated with reduced cell-growth and induction of apoptosis (Mitchell et al., 1999).

It is of clear interest that resveratrol not only downregulated the AR in our TRAP model but also suppressed the androgen responsive gene, Gk11, known as the ortholog of human PSA, at the mRNA level. This *in vivo* finding reflect that resveratrol suppressed AR pathway functionally in prostatic lesions of TRAP rats that might similar to affect PSA in human condition, such as the effect of anti-androgen drugs suppressed PSA level that paralleled with cancer growth inhibition by interrupting AR signal pathways in prostate cancer patients.

Resveratrol is also known to suppress late stage processes of carcinogenesis such as angiogenesis and metastasis. For example, resveratrol was able to directly inhibit the gelatinolytic activities of MMP2 and MMP9 which are associated with tumor metastasis (Banerjee et al., 2002). However, effects in cell culture may not directly reflect whole body systems in animal systems and administration of 1-5 mg per kg (body weight) daily of resveratrol in one study failed to affect the growth or metastasis of breast cancer in mice, despite promising *in vitro* results (Bove et al., 2002). In the present investigation, resveratrol similarly did not reduce lung metastasis in mice bearing prostate carcinoma tumors, possibly because the PLS30 cells used are negative for AR protein and show and androgen-independent

phenotype (Nakanishi et al., 1996). Thus, effects of resveratrol are more likely to be AR-dependent. Understanding the molecular mechanisms of resveratrol mediated downregulation of AR signaling may aid in the development of effective chemoprevention since the receptor plays a major role in the initiation and progression of prostate cancer (Sadi et al., 1991). The observed unique effects of resveratrol on AR protein point to possible optimization of chemopreventive effect in future by use in combination with other agents such as vitamin E (Zhang et al., 2002) and selenium (Chun et al., 2006).

In conclusion, our *in vivo* results clearly demonstrated that resveratrol can inhibit prostate carcinogenesis with induction of apoptosis through AR down-regulation, without any signs of tissue-toxicity. Our findings provide support for previous in vitro data as well as population-based case-control study suggesting that resveratrol intake through wine associated with the reduction of the relative risk of prostate cancer. Our findings and the fact that most prostate cancers are initially androgen-dependent suggest that resveratrol warrants further examination with the eventual aim of clinical testing.

Acknowledgments

This work was supported by a Grant-in-Aid for Cancer Research from the Ministry of Health, Labour and Welfare of Japan, a Grant-in-Aid for the 2nd Term Comprehensive 10-Year Strategy for Cancer Control from the Ministry of Health, Labour and Welfare of Japan, a grant from the Japan Food Chemical Research Foundation, and a grant from the Society for Promotion of Pathology of Nagoya, Japan.

References

Asamoto M, Hokaiwado N, Cho YM, et al (2001a). Prostate carcinomas developing in transgenic rats with SV40 T antigen expression under probasin promoter control are strictly androgen dependent. *Cancer Res*, **61**, 4693-700.

Asamoto M, Hokaiwado N, Cho YM, et al (2001b). Metastasizing neuroblastomas from taste buds in rats transgenic for the Simian virus 40 large T antigen under control of the probasin gene promoter. *Toxicol Pathol*, **29**, 363-8.

Asamoto M, Hokaiwado N, Cho YM, et al (2002). Effects of genetic background on prostate and taste bud carcinogenesis due to SV40 T antigen expression under probasin gene promoter control. *Carcinogenesis*, **23**, 463-7.

Aggarwal BB, Bhardwaj A, Aggarwal RS, et al (2004). Role of resveratrol in prevention and therapy of cancer: preclinical and clinical studies. *Anticancer Res*, **24**, 2783-840.

Aziz MH, Kumar R, Ahmad N (2003). Cancer chemoprevention by resveratrol: in vitro and in vivo studies and the underlying mechanisms (review). *Int J Oncol*, **23**, 17-28.

Baur JA, Sinclair DA (2006). Therapeutic potential of resveratrol: the in vivo evidence. *Nat Rev Drug Discov*, **5**, 493-506.

Baur JA, Pearson KJ, Price NL, et al (2006). Resveratrol improves health and survival of mice on a high-calorie diet. *Nature*, **444**, 337-42.

Banerjee S, Bueso-Ramos C, Aggarwal BB (2002). Suppression of 7,12-dimethylbenz(a)anthracene-induced mammary carcinogenesis in rats by resveratrol: role of nuclear factor-kappaB, cyclooxygenase 2, and matrix metalloprotease 9. *Cancer Res*, **62**, 4945-54.

Bhat KP, Pezzuto JM (2002). Cancer chemopreventive activity of resveratrol. *Ann N Y Acad Sci*, **957**, 210-29.

Bove K, Lincoln DW, Tsan MF (2002). Effect of resveratrol on growth of 4T1 breast cancer cells in vitro and in vivo. *Biochem Biophys Res Commun*, **291**, 1001-5.

Cho YM, Takahashi S, Asamoto M, et al (2003). Age-dependent histopathological findings in the prostate of probasin/SV40 T antigen transgenic rats: lack of influence of carcinogen or testosterone treatment. *Cancer Sci*, **94**, 153-7.

Chun JY, Nadiminty N, Lee SO, et al (2006). Mechanisms of selenium down-regulation of androgen receptor signaling in prostate cancer. *Mol Cancer Ther*, **5**, 913-8.

Delmas D, Lancon A, Colin D, et al (2006). Resveratrol as a chemopreventive agent: a promising molecule for fighting cancer. *Curr Drug Targets*, **7**, 423-42.

Friel H, Lederman H (2006). A nutritional supplement formula for influenza A (H5NCancer Epidemiol Biomarkers Prev, 16, 2193-2203.Cancer Epidemiol Biomarkers Prev, 16, 2193-2203) infection in humans. *Med Hypotheses*, **67**, 578-87.

Gescher AJ, Steward WP (2003). Relationship between mechanisms,bioavailibility, and preclinical chemopreventive efficacy of resveratrol: a conundrum. *Cancer Epidemiol Biomarkers Prev*, **12**, 953-7.

Hsieh TC, Wu JM (2000). Grape-derived chemopreventive agent resveratrol decreases prostate-specific antigen (PSA) expression in LNCaP cells by an androgen receptor (AR)-independent mechanism. *Anticancer Res*, **20**, 225-8.

Jang M, Cai L, Udeani GO, et al (1997). Cancer chemopreventive activity of resveratrol, a natural product derived from grapes. *Science*, **275**, 218-20.

Jemal A, Siegel R, Ward E, et al (2007). Cancer statistics. *CA Cancer J Clin*, **57**, 43-66.

Jones SB, DePrimo SE, Whitfield ML, et al (2005). Resveratrol-induced gene expression profiles in human prostate cancer cells. *Cancer Epidemiol Biomarkers Prev*, **14**, 596-604.

Juan ME, Vinardell MP, Planas JM (2002). The daily oral administration of high doses of trans-resveratrol to rats for 28 days is not harmful. *J Nutr*, **132**, 257-60.

Kandori H, Suzuki S, Asamoto M, et al (2005). Influence of atrazine administration and reduction of calorie intake on prostate carcinogenesis in probasin/SV40 T antigen transgenic rats. *Cancer Sci*, **96**, 221-6.

Kato K, Takahashi S, Mori T et al (1998). Establishment of transplantable rat prostate carcinomas from primary lesions induced by 3,2'-dimethyl-4-aminobiphenyl and testosterone. *J Toxicol Pathol*, **11**, 27-32.

Kyprianou N, Isaacs JT (1988). Activation of programmed cell death in the rat ventral prostate after castration. *Endocrinology*, **122**, 552-62.

Lagouge M, Argmann C, Gerhart-Hines Z, et al (2006). Resveratrol improves mitochondrial function and protects against metabolic disease by activating SIRT1 and PGC-1alpha. *Cell*, **127**, 1109-22.

Mitchell SH, Zhu W, Young CY (1999). Resveratrol inhibits the expression and function of the androgen receptor in LNCaP prostate cancer cells. *Cancer Res*, **59**, 5892-5.

Nakanishi H, Takeuchi S, Kato K, et al (1996). Establishment and characterization of three androgen-independent, metastatic carcinoma cell lines from 3,2'-dimethyl-4-aminobiphenyl-induced prostatic tumors in F344 rats. *Jpn J Cancer Res*, **87**, 1218-26.

Palamara AT, Nencioni L, Aquilano K, et al (2005). Inhibition of influenza A virus replication by resveratrol. *J Infect Dis*, **191**, 1719-29.

Sadi MV, Walsh PC, Barrack ER (1991). Immunohistochemical study of androgen receptors in metastatic prostate cancer. Comparison of receptor content and response to hormonal therapy. *Cancer*, **67**, 3057-64.

Said MM, Hokaiwado N, Tang M, et al (2006). Inhibition of prostate carcinogenesis in probasin/SV40 T antigen transgenic rats by leuprorelin, a luteinizing hormone-releasing hormone agonist. *Cancer Sci*, **97**, 459-67.

Schoonen WM, Salinas CA, Kiemeney LA, et al (2005). Alcohol consumption and risk of prostate cancer in middle-aged men. *Int J Cancer*, **113**, 133-40.

Stewart JR, Artime MC, O'Brian CA (2003). Resveratrol: a candidate nutritional substance for prostate cancer prevention. *J Nutr*, **133**, 2440S-3S.

Sporn MB, Suh N (2002). Chemoprevention: an essential approach to controlling cancer. *Nat Rev Cancer*, **2**, 537-43.

Syed DN, Khan N, Afaq F, et al (2007). Chemoprevention of prostate cancer through dietary agents: Progress and promise.

Tang M, Ogawa K, Asamoto M, et al (2007). Protective effects of citrus nobiletin and auraptene in transgenic rats developing adenocarcinoma of the prostate (TRAP) and human prostate carcinoma cells. *Cancer Sci*, **98**, 471-7.

Tsao AS, Kim ES, Hong WK (2004). Chemoprevention of cancer. *CA Cancer J Clin*, **54**, 150-80.

Valenzano DR, Terzibasi E, Genade T, et al (2006). Resveratrol prolongs lifespan and retards the onset of age-related markers in a short-lived vertebrate. *Curr Biol*, **16**, 296-300.

Vitaglione P, Sforza S, Galaverna G, et al (2005). Bioavailability of trans-resveratrol from red wine in humans. *Mol Nutr Food Res*, **49**, 495-504.

Wexler H (1966). Accurate identification of experimental pulmonary metastases. *J Natl Cancer Inst*, **36**, 641-5.

Zeng Y, Yokohira M, Saoo K, et al (2005). Inhibition of prostate carcinogenesis in probasin/SV40 T antigen transgenic rats by raloxifene, an antiestrogen with anti-androgen action, but not nimesulide, a selective cyclooxygenase-2 inhibitor. *Carcinogenesis*, **26**, 1109-16.

Zhang Y, Ni J, Messing EM, et al (2002). Vitamin E succinate inhibits the function of androgen receptor and the expression of prostate-specific antigen in prostate cancer cells. *Proc Natl Acad Sci USA*, **99**, 7408-13.

The Prostate 69:644–651 (2009)

Suppression of Prostate Cancer in a Transgenic Rat Model Via γ-Tocopherol Activation of Caspase Signaling

Satoru Takahashi,[1]* Kentaro Takeshita,[1] Azman Seeni,[1] Satoshi Sugiura,[1] Mingxi Tang,[1] Shin-ya Sato,[1] Hiroki Kuriyama,[2] Masao Nakadate,[2] Koichi Abe,[3] Yoshitaka Maeno,[4] Masataka Nagao,[4] and Tomoyuki Shirai[1]

[1]*Department of Experimental Pathology and Tumor Biology, Mizuho-ku, Nagoya, Japan*
[2]*Tama Biochemical Co. Ltd, Isehara, Kanagawa, Japan*
[3]*Eisai Co. Ltd., Bunkyo-ku, Tokyo, Japan*
[4]*Forensic Medical Science, Nagoya City University Graduate School of Medical Sciences, Nagoya, Japan*

BACKGROUND. Epidemiological data indicate that intake of one form of vitamin E, γ-tocopherol, may reduce prostate cancer risk, and several in vitro studies have demonstrated that γ-tocopherol can inhibit prostate cancer cell growth. The purpose of the present study was to confirm effects of γ-tocopherol on prostate cancer in the transgenic rat for adenocarcinoma of prostate (TRAP) model established in our laboratory.

METHODS. In Experiment 1, heterozygous male TRAP rats 5 weeks of age received α-tocopherol at the concentration of 50 mg/kg in the diet, or γ-tocopherol at 50 or 100 mg/kg for 10 weeks. In Experiment 2, TRAP rats of 3 weeks of age were given γ-tocopherol at 50, 100, or 200 mg/kg diet for 7 weeks.

RESULTS. γ-Tocopherol did not affect body weight gain, organ weights or serum levels of either testosterone or estradiol. However, quantitative evaluation of prostatic lesions demonstrated significantly suppression of sequential progression from PIN to adenocarcinoma in a dose-dependent manner, along with clear activation of caspases 3 and 7 in the ventral lobe in both experiments.

CONCLUSIONS. The present study clearly demonstrated that γ-tocopherol suppresses prostate tumor progression in an in vivo TRAP model, and could be a candidate chemopreventive agent for human prostate cancer. *Prostate 69: 644–651, 2009.* © 2009 Wiley-Liss, Inc.

KEY WORDS: **γ-tocopherol; prostate cancer; transgenic rat model, chemoprevention**

INTRODUCTION

Prostate cancer has become the most common malignancy in men in Europe and the United States while its incidence remains relatively low in Asian countries [1]. It has been estimated there were approximately 232,090 new cases of prostate cancer and 30,350 deaths from prostate cancer in the United States in 2005 [2]. Prevalence of prostate cancer has also been increasing in Japan [3], concomitantly with change in life style. Androgen ablation therapy is widely accepted and carried out for prostate cancers because androgens are essential for the development and growth of normal prostate and prostate cancer cells

Azman Seeni's present address is School of Dental Sciences, Universiti Sains Malaysia, 16150 Kubang Kerian, Kelantan, Malaysia.

Masataka Nagao's present address is Department of Legal Medicine, Graduate School of Biomedical Sciences, Hiroshima University, Hiroshima, Japan.

*Correspondence to: Satoru Takahashi, 1 Kawasumi, Mizuho-cho, Mizuho-ku, Nagoya 467-8601, Japan.
E-mail: sattak@med.nagoya-cu.ac.jp
Received 25 September 2008; Accepted 5 December 2008
DOI 10.1002/pros.20915
Published online 13 January 2009 in Wiley InterScience (www.interscience.wiley.com).

[4]. However, outgrowth of hormone-independent cancer cells occurs within 1–2 years and eventually leads to a fatal outcome in many cases [5].

Chemoprevention is one attractive approach for prostate cancer because of the high population incidence and long latent period, and several dietary factors as well as genetic background have been linked to risk and progression of prostate cancer [6–8]. Prostate cancer is known to be strongly associated with aging, that is, about three-quarters of cases worldwide occur in men aged 65 years or more [1]. Therefore, the main strategy with chemoprevention for prostate cancer is to delay the development of clinically evident disease due to suppression of progression from precancerous lesions to invasive cancer. Many observational or intervention studies have been conducted using vitamins, phytochemicals and minerals [5]. α- and γ-Tocopherols, forms of vitamin E, are nutritional elements that may reduce risk of prostate cancer [9–13]. To confirm effects of γ-tocopherol in vivo, we here performed animal experiments using the transgenic rat for adenocarcinoma of prostate (TRAP) model that features development of high-grade prostatic intraepithelial neoplasia (PIN) from 4 weeks of age and well—moderately differentiated adenocarcinomas with high incidences by 15 weeks of age [14,15]. These characteristics of TRAP have been shown to be very suitable for evaluation of strategies for chemoprevention and treatment [16–19].

MATERIALS AND METHODS

Chemicals and Animals

Vitamin E-free, α- or γ-tocopherol-contained diets were donated by Tama Biochemical Co. Ltd. (Japan). Antibodies for caspases 3, 6, 7, 9, cleaved caspases 3, 7, Erk1/2, phospho-Erk1/2, p38 MAPK, phospho-p38 MAPK, SAPK/JNK, and phospho-SAPK/JNK were purchased from Cell Signaling Technology (Beverly, MA). Anti-AR (PG-21) was from Upstate Technology (Lake Placid, NY, CA), anti-cyclin D1 was from Oncogene Research Product, anti-Bcl-xL was from Pharmingen, anti-SV40T Ag was from Santa Cruz Biotechnology, Inc. and anti-β-actin was from Sigma–Aldrich, Inc. Male heterozygous TRAP rats with a Sprague–Dawley genetic background were bred in our animal facility for use in the present study. They were housed 2–3/cage on wood-chip bedding in an air-conditioned animal room at 23 ± 2°C and 50 ± 10% humidity. Food and tap water were available ad libitum.

Experimental Protocol

Experiment 1. A total of 40 male TRAP rats aged 5 weeks were randomly divided into four groups. Rats of group 1 as a control received vitamin E-free AIN73 basal diet. The rats of groups 2–4 continuously received α-tocopherol at the concentration of 50 mg/kg diet, or γ-tocopherol at the concentrations of 50 or 100 mg/kg diet for 10 weeks, respectively. The experiment was terminated at week 10.

Experiment 2. A total of 56 heterozygous male TRAP rats aged 3 weeks were randomly divided into four groups. Rats of group 1 served as a control receiving vitamin E-free AIN73 basal diet. The rats of groups 2, 3, and 4 continuously received γ-tocopherol-containing AIN73 at the concentrations of 50, 100, or 200 mg/kg diet for 7 weeks, respectively. The experiment was terminated at week 7.

In both experiments, prostates were removed and fixed in formalin. Portions were immediately frozen in liquid nitrogen and stored at −80°C until processed. Testosterone and estrogen levels in serum were analyzed using radioimmunoassays by a commercial laboratory (SRL, Inc., Tokyo, Japan). The present experiments were performed under protocols approved by the Institutional Animal Care and Use Committee of Nagoya City University Graduate School of Medical Sciences.

Assessment of Prostate Neoplastic Lesion Development

Neoplastic lesions in prostate glands of TRAP rats were evaluated as previously described [18]. Briefly, neoplastic lesions were classified into three types; low-grade PIN (LG-PIN), high-grade PIN (HG-PIN) and adenocarcinoma. The relative numbers of acini with the relevant histological characteristics were quantified by counting, the results being expressed relative to the total acini in each prostatic lobe.

Immunoblot Analysis

Frozen ventral prostate tissues were homogenized in RIPA buffer (150 mM NaCl, 50 mM Tris–HCl (pH 8.0), 1% NP-40, 0.5% sodium deoxycholate, 0.1% SDS, 1 mM phenylmethylsulphonyl fluoride, 1 mM sodium orthovanadate, and protease inhibitor cocktail (Complete, Roche)). Twenty microgram aliquots of protein were resolved on SDS–PAGE and separated proteins were transferred to nitrocellulose membranes for detection with horseradish peroxidase conjugated secondary antibodies and the ECL Plus system (Amersham Pharmacia Biotech).

Determination of Total Ceramide Content

The frozen tissues of ventral prostates were homogenized in twenty parts of chloroform/methanol (2:1) containing 250 ng of C_2-ceramide as an internal

standard and extracted for 30 min on ice. After centrifugation, the chloroform phase was dried under a nitrogen stream. The amount of C_{16}-ceramide in tissue was quantified by high-performance liquid chromatography/electro-spray ionization mass spectrometry (LC/MS) as described by Soeda et al. [20].

HPLC Method for the Determination of Tocopherols in Rat Plasma

Tocopherols are extracted from 0.5 ml of plasma with 5.0 ml of n-hexane after addition of 0.7 ml of water and 1.0 ml of ethanol containing dl-Tocol (3.92 μg/ml) as an internal standard. Hexane extracts (4 ml) are evaporated under a nitrogen stream at 40°C and residues were dissolved in 100 μl aliquots of n-Hexane. The resultant solutions were applied to a high-performance liquid chromatography column (Nucleosil-100 Å 5 μm NH2, 4.6 mm × 250 mm; elution, n-Hexane/isopropyl alcohol = 98:2).

Immunohistochemistry

For Ki-67 immunostaining, deparaffinized sections were incubated with diluted rabbit polyclonal Ki-67 antibodies (Novocastra, New Castle, UK). Apoptotic cells were detected using an In situ Apoptosis Detection Kit (TUNEL method) according to the manufacturer's instructions (Takara Bio Co. Ltd, Japan). Labeling indices were counted separately in the ventral, dorsal and lateral prostate and expressed as numbers of Ki-67-positive or TUNEL-positive cells per 100 cells.

Statistical Analysis

Differences in means between groups were determined by analysis of variance (ANOVA), followed by the Scheffe's post-hoc test with StatView (version 5.0) software (SAS Institute, Inc., Cary, NC). The Spearman's rank correlation coefficient test was used for analysis of dependent data.

RESULTS

Experiment I

α- and γ-Tocopherol did not influence the mean body weights and relative liver and ventral prostate weights (Table I). Serum levels of testosterone and estradiol were also not affected (Fig. 1A). There were partial pathological responses to γ-tocopherol as demonstrated by reduction in the prostatic neoplastic lesions in TRAP rats (Fig. 1B). However, small foci of adenocarcinoma still remained, so that there were no significant differences in the incidences of PIN or adenocarcinomas in the prostates of TRAP rats. Quantitative evaluation of the proportion of preneoplastic and neoplastic lesions in prostate glands showed γ-tocopherol to significantly suppress progression from PIN to adenocarcinoma in a dose-dependent manner in the ventral lobe while α-tocopherol was without apparent influence (Table II). In the lateral lobe, γ-tocopherol treatment also tended to suppress progression but this was not significant. Immunoblot analyses showed activation of caspases 3 and 7, inactivation of Erk1/2 and decreased expression of bcl-2 in the ventral prostate of rats treated with γ-tocopherol while expression of cyclin D1 and SV40 T antigen did not differ among the groups (Fig. 2). There was no variation in ceramide content in the ventral prostate among the groups (Fig. 1C).

Experiment 2

To confirm the reproducibility of the suppressive effects of γ-tocopherol on prostate carcinogenesis, we performed a similar experiment as in Experiment 1. γ-Tocopherol did not affect either body weight gain or organ weights (Table III). Serum levels of testosterone and estradiol again did not differ among the groups (Fig. 3A). Serum concentrations of γ-tocopherol were increased in a dose-dependent manner while the α-tocopherol level was not affected (Fig. 3B). Prostate adenocarcinomas were found only in ventral and lateral lobes and no intergroup differences in incidences were observed. However, progressive

TABLE I. Final Body and Relative Organ Weights (Experiment I)

Treatment	No. of rats	Body weight (g)	Relative organ weight (%)	
			Liver	Ventral prostate
Control	10	463.7 ± 34.7	3.27 ± 0.24	0.056 ± 0.014
α-Tocopherol 50 mg/kg	10	448.6 ± 40.1	3.22 ± 0.15	0.064 ± 0.007
γ-Tocopherol 50 mg/kg	10	455.0 ± 28.9	3.39 ± 0.21	0.060 ± 0.009
γ-Tocopherol 100 mg/kg	10	445.7 ± 39.0	3.47 ± 0.28	0.060 ± 0.008

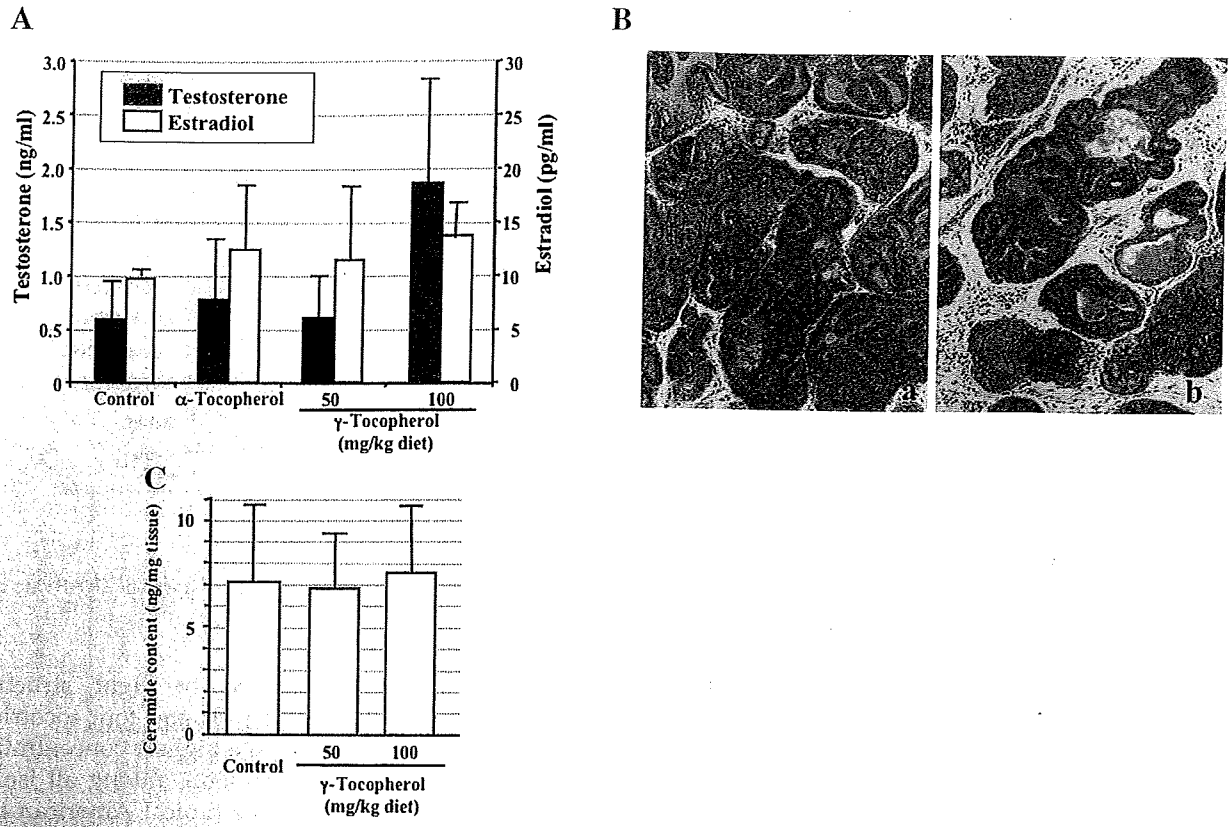

Fig. 1. Effects of γ-tocopherol on serum steroid hormones, prostatic lesions and ceramide content in prostate glands in Experiment I. **A**: Serum levels of testosterone and estradiol. **B**: Representative histopathological findings for lesions in the ventral prostates of the controls (a) and the 100 mg/kg γ-tocopherol group (b). **C**: Ceramide contents in ventral prostates.

changes of prostatic lesions showed a significant suppression by γ-tocopherol in a dose-dependent manner in the ventral but not the lateral lobe (Table IV). The numbers of apoptotic cells in the ventral prostate of rats treated with γ-tocopherol were significantly increased in a dose-dependent manner as compared with the controls whereas there were no obvious differences in Ki-67 labeling indices (Fig. 3C,D). Immunoblot analyses clearly demonstrated activation of caspases 3 and 7 and a tendency for inactivation of Erk1/2 in the ventral prostate of rats treated with γ-tocopherol (Fig. 4).

TABLE II. Quantitative Evaluation of Neoplastic Lesions in Prostates of TRAP Rats Treated With α- and γ-Tocopherol (Experiment I)

Treatment	No. of rats	Relative number of acini with histological characteristics (%)					
		Ventral lobe			Lateral lobe		
		LG-PIN	HG-PIN	ADC	LG-PIN	HG-PIN	ADC
Control	10	5.4 ± 2.5	87.5 ± 2.4	7.2 ± 2.3	14.2 ± 3.9	84.4 ± 3.6	1.4 ± 1.3
α-Tocopherol 50 mg/kg	10	8.6 ± 2.9	85.4 ± 1.8	6.0 ± 1.9	16.5 ± 8.7	82.3 ± 8.3	1.2 ± 0.9
γ-Tocopherol 50 mg/kg	10	8.1 ± 3.1	86.9 ± 3.5	5.0 ± 1.8[b]	19.4 ± 6.5	79.9 ± 6.7	0.7 ± 0.8
γ-Tocopherol 100 mg/kg	10	9.8 ± 4.9	85.4 ± 4.4	4.7 ± 1.0[a,b]	15.9 ± 5.8	83.5 ± 5.8	0.6 ± 0.7

LG-PIN, low grade prostatic intraepithelial neoplasia; HG, high grade; ADC, adenocarcinoma.
[a] $P < 0.05$ versus control.
[b] $P < 0.01$ versus control (Spearman's rank correlation coefficient test).

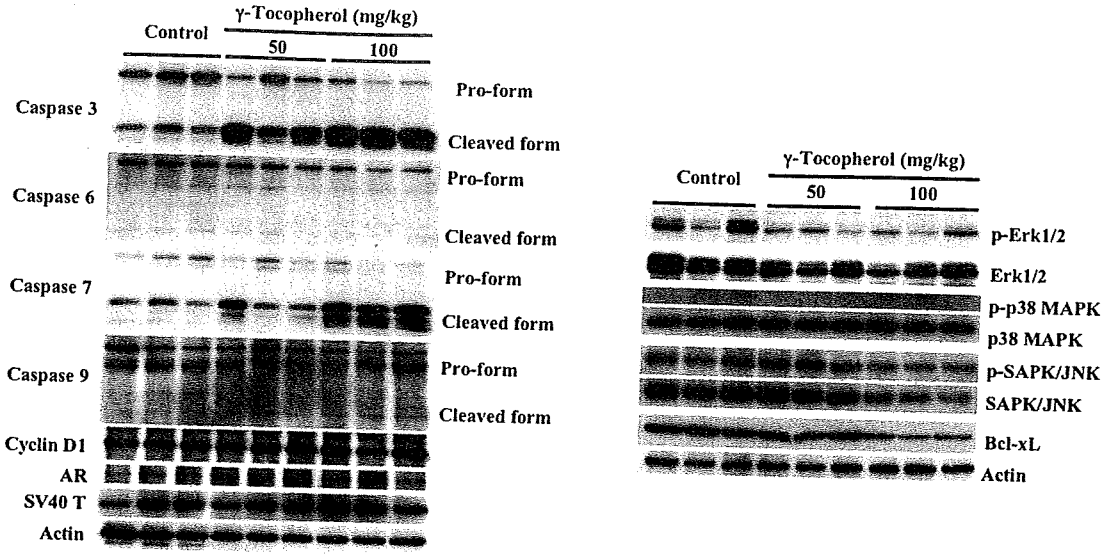

Fig. 2. Results of immunoblot analysis of caspases, MAPKs and other apoptosis-related proteins in ventral prostates of TRAP rats treated with γ-tocopherol in Experiment I.

DISCUSSION

To our knowledge, this is the first study to demonstrate suppression effects of γ-tocopherol on prostate tumor progression in an in vivo animal model. Various mechanisms whereby the compound could inhibit prostate cancer cell growth have been indicated in in vitro studies, including downregulation of cyclins D1 and E [21,22] or induction of apoptosis by interrupting sphingolipid synthesis [23]. The data from our TRAP model also point to induction of apoptosis via activation of caspases 3 and 7 by γ-tocopherol although downregulation of cyclin D1 and significant accumulation of ceramide were not found.

It has been reported that Japanese men intake an average of 12.2 ± 2.1 mg γ-tocopherol per day in daily life [24]. The amount of γ-tocopherol used in the highest-dose group (200 mg/kg diet) of present study was 50–60 times higher than this human exposure level and was equivalent to an intake of 950 mg/day by a 70 kg-sized human. However, it is possible to consume this amount of γ-tocopherol in nutritional supplements.

Vitamin E is composed of eight structurally related forms, four tocopherols and four tocotrienols. α-Tocopherol is found as the highest concentration in serum and dietary supplements among all isoforms but the primary form in the typical American diet is γ-tocopherol, which is present at 2–4 times higher concentrations than α-tocopherol [25]. Although both α- and γ-tocopherol are potent antioxidants, γ-tocopherol has a unique function due to its different chemical structure that scavenges reactive nitrogen species that damage proteins, lipids, and DNA. Therefore, γ-tocopherol possesses electrophile-trapping and nitrogen dioxide-radical-trapping properties that are different from those of α-tocopherol [26,27]. Consequently, γ-tocopherol appears to have greater efficacy than α-tocopherol at inhibiting lipid peroxidation under nitration system conditions [28]. Furthermore, γ-tocopherol but not α-tocopherol exhibits anti-inflammatory activities by inhibiting cyclooxygenase-catalyzed prostaglandin E_2 formation in cell culture and in animals in vivo [29,30]. Recent clinical trials revealed no significant reduction of overall cardiovascular events or cancer by α-tocopherol

TABLE III. Final Body and Relative Organ Weights (Experiment 2)

Treatment	No. of rats	Body weights (g)	Relative organ weights (%)			
			Liver	Kidneys	Heart	Ventral prostate
Control	14	347.5 ± 42.4	4.06 ± 0.29	0.68 ± 0.03	0.32 ± 0.01	0.065 ± 0.009
γ-Tocopherol 50 mg/kg	14	353.3 ± 35.9	4.18 ± 0.30	0.70 ± 0.04	0.33 ± 0.02	0.066 ± 0.010
γ-Tocopherol 100 mg/kg	14	343.5 ± 41.1	3.97 ± 0.24	0.69 ± 0.03	0.33 ± 0.01	0.063 ± 0.007
γ-Tocopherol 200 mg/kg	14	340.5 ± 27.0	3.86 ± 0.31	0.69 ± 0.04	0.33 ± 0.02	0.060 ± 0.009